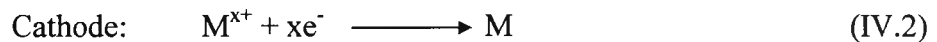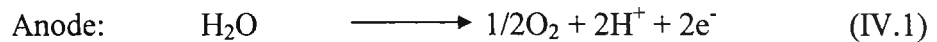# CHAPTER IV

METAL RECOVERY BY ELECTRODEPOSITION
TECHNIQUE

1. Copper recovery

1.1 Copper recovery in classical reactor without membrane

Electrodeposition is the procedure to deposit metal ions contained in electrolyte on the cathode surface by electricity. The reaction occurs when a current is applied to the system. An oxidation reaction is observed at anode and consequently releases oxygen gas whereas a reduction reaction is observed at cathode. Metal ions containing in a solution deposit on a cathode surface in metallic form. The main reactions observed at both electrodes are expressed by the following reactions.

$$\text{Anode:} \qquad H_2O \qquad \longrightarrow \qquad 1/2O_2 + 2H^+ + 2e^- \qquad \text{(IV.1)}$$

$$\text{Cathode:} \qquad M^{x+} + xe^- \qquad \longrightarrow \qquad M \qquad \text{(IV.2)}$$

M is corresponding to a metal (Cu, Zn and so on.).

Parameters affecting the electrodeposition process are applied current density, electrolysis time, electrolyte flow rate, metal concentrations, and chemical and physical properties of electrolyte.

1.1.1 Influence of current density

The results of copper recovery from synthetic copper solution with 1 g/l concentration at pH = 1 (solution S1) by applying various current densities (from 5 to 25 A/m^2) are presented in Figure IV.1. The optimum current density corresponding to the maximum current efficiency was found at 10 A/m^2 as shown in Figure IV.2. More than 90 % of copper was recovered in 6 hours and the current efficiency at the optimum current density was more than 90 % at 70 % recovery. When the current density is less than optimum current density, their current efficiency was nearly the same but operating time is increased. However, when the current density increased,

the current efficiency sharply decreased at all percentages of copper recovery. This results from the loss of current due to a side reaction such as production reaction of hydrogen gas.
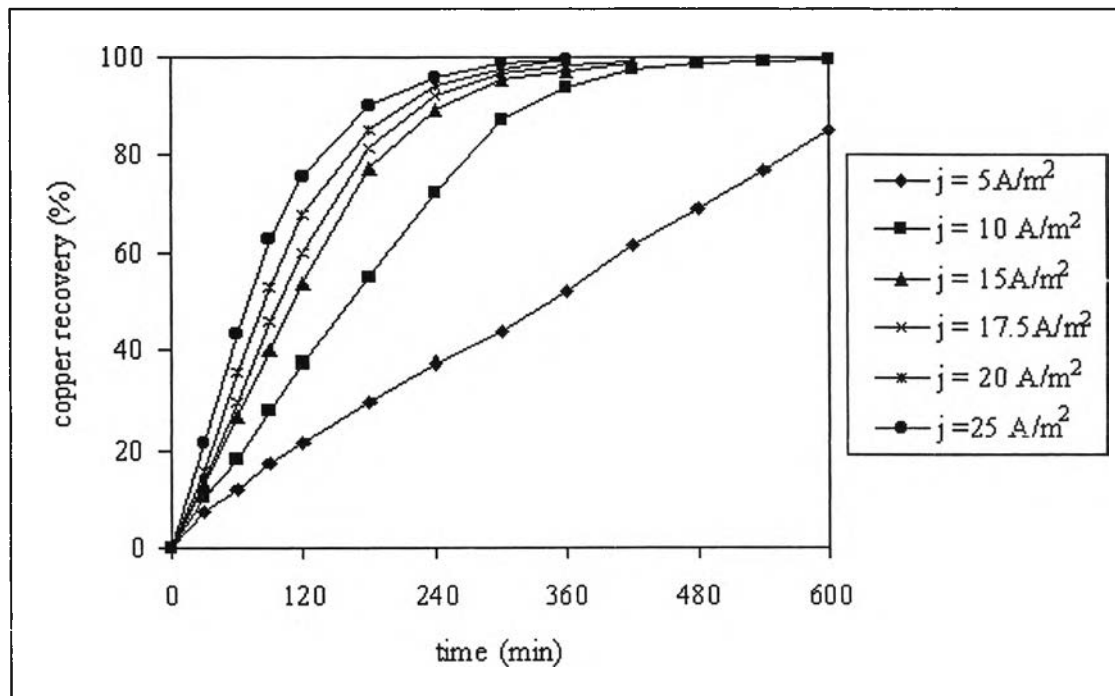

Figure IV.1: Copper recovery percentage versus time (solution S1).
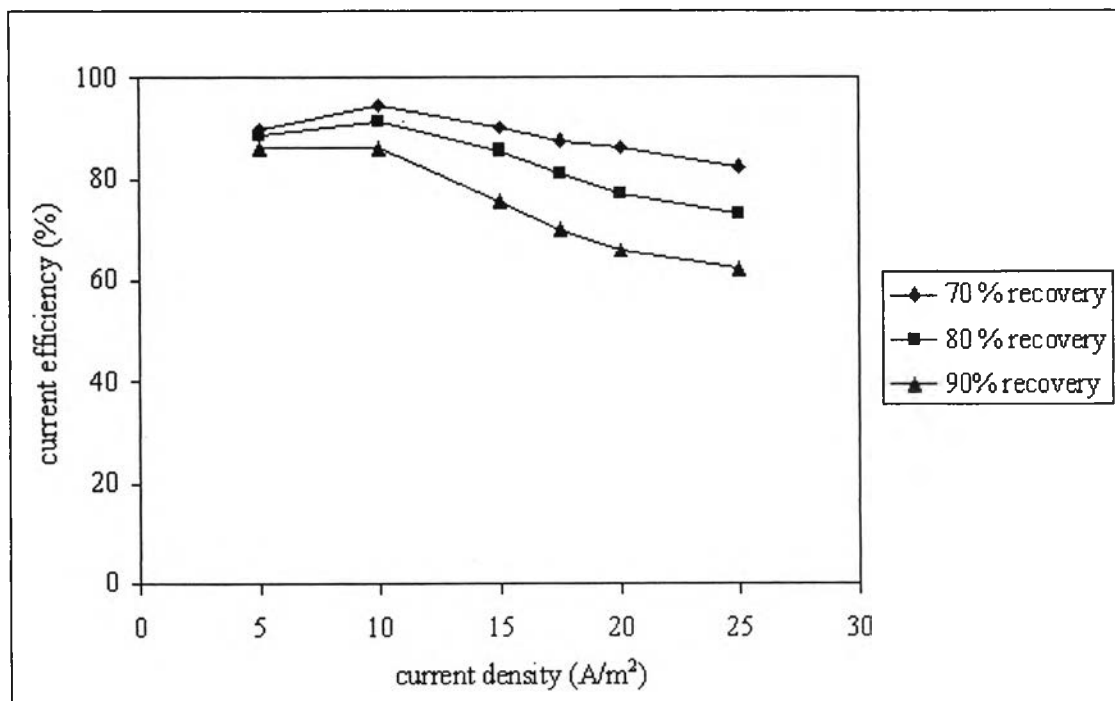

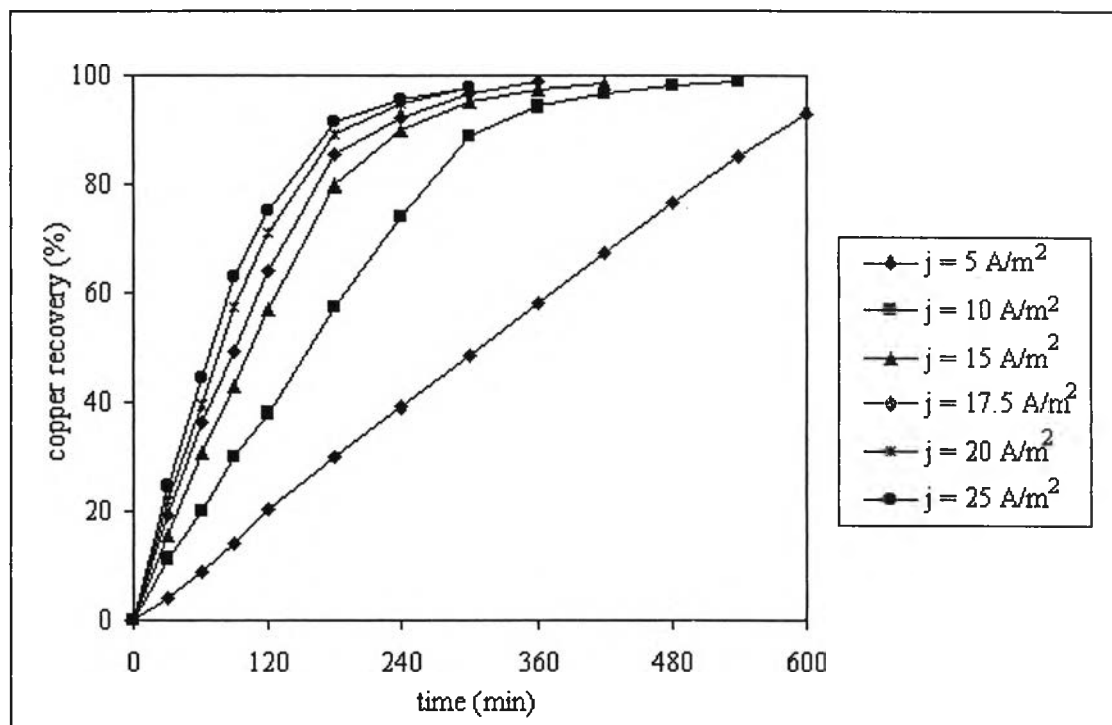Figure IV.2: Current efficiency versus current density (solution S1).

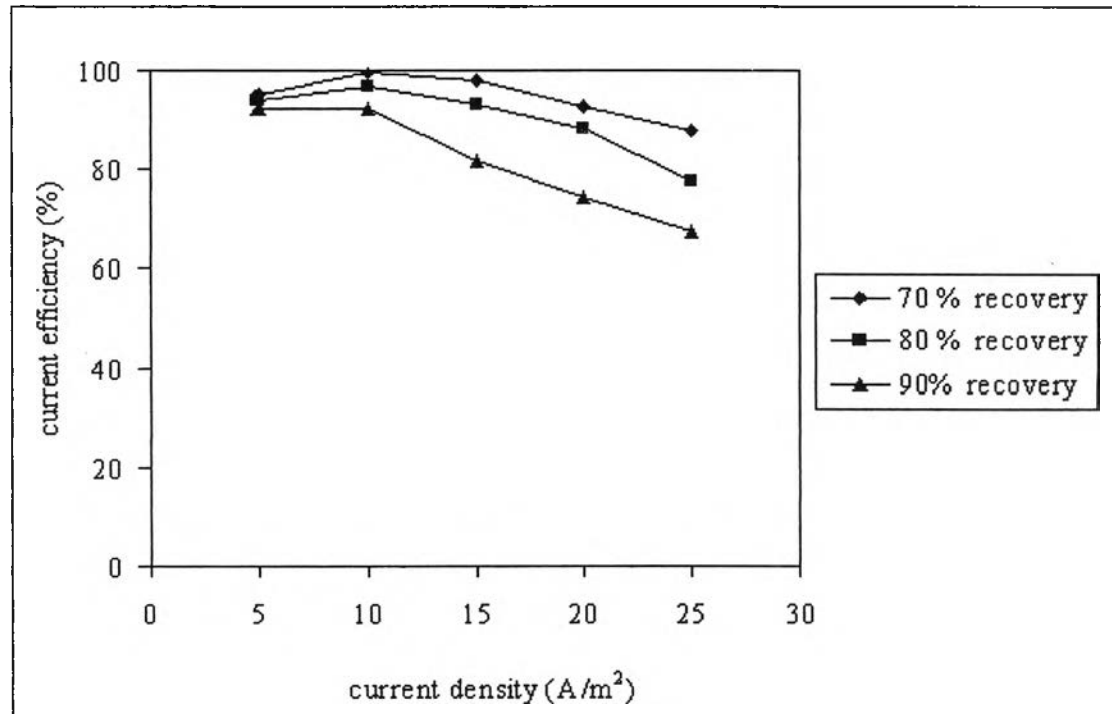Figure IV.3: Copper recovery percentage versus time (solution S2).

Figure IV.4: Current efficiency versus current density (solution S2).

Figures IV.3 and IV.4 illustrate the results of copper recovery from the synthetic aqueous solution with concentration of 1 g/l at pH = 5 (solution S2) when holding the same current density range. It seems that more than 90 % of copper were recovered in 6 hours in current density range from 10 to 25 A/m^2. The optimum current density was quite as same as that obtained at lower pH, it was found at 10 A/m^2. From these results, it could be concluded that pH did not affect to a copper deposition. Figure IV.5 is a plot of metal concentration evolution versus time for solutions S1 and S2. It showed that the concentration evolutions obtained from the synthetic solutions at pH = 1 and pH = 5 were nearly identical. A few deviations were observed at an initial electrolysis time (during 0 - 100 minutes) because initial concentrations of metal were different (about 2.3 %).
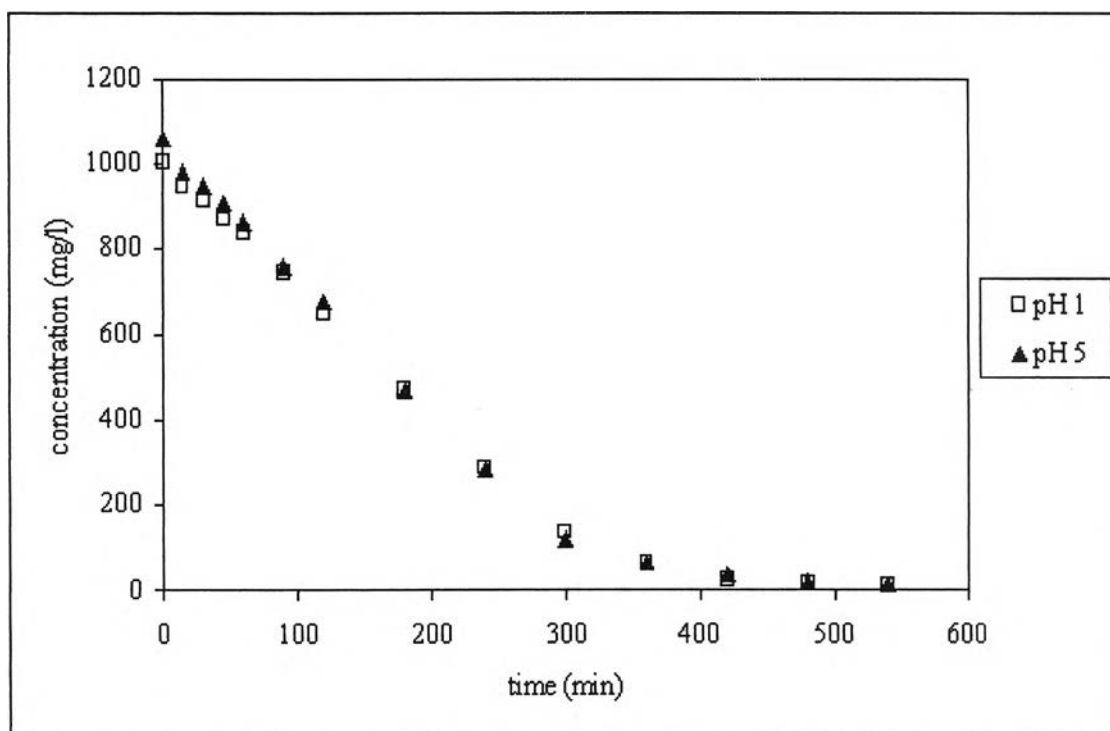

Figure IV.5: Concentration evolution versus time of solutions S1 and S2
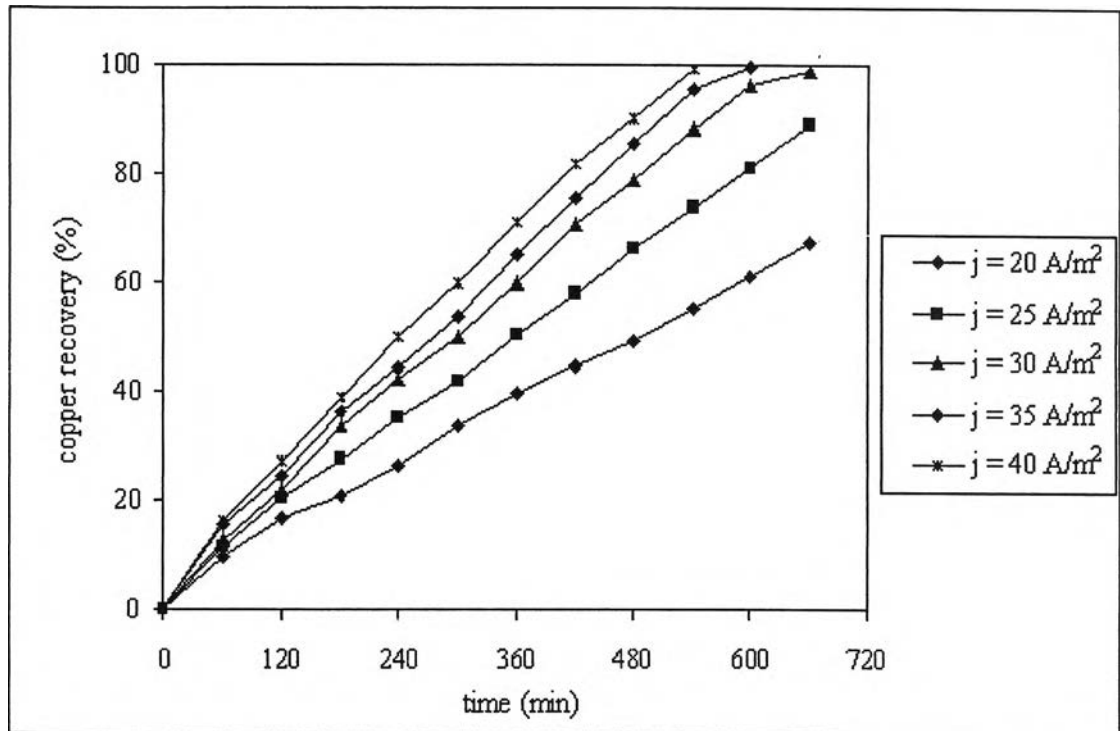at 10 A/m^2 and 0.42 l/min.

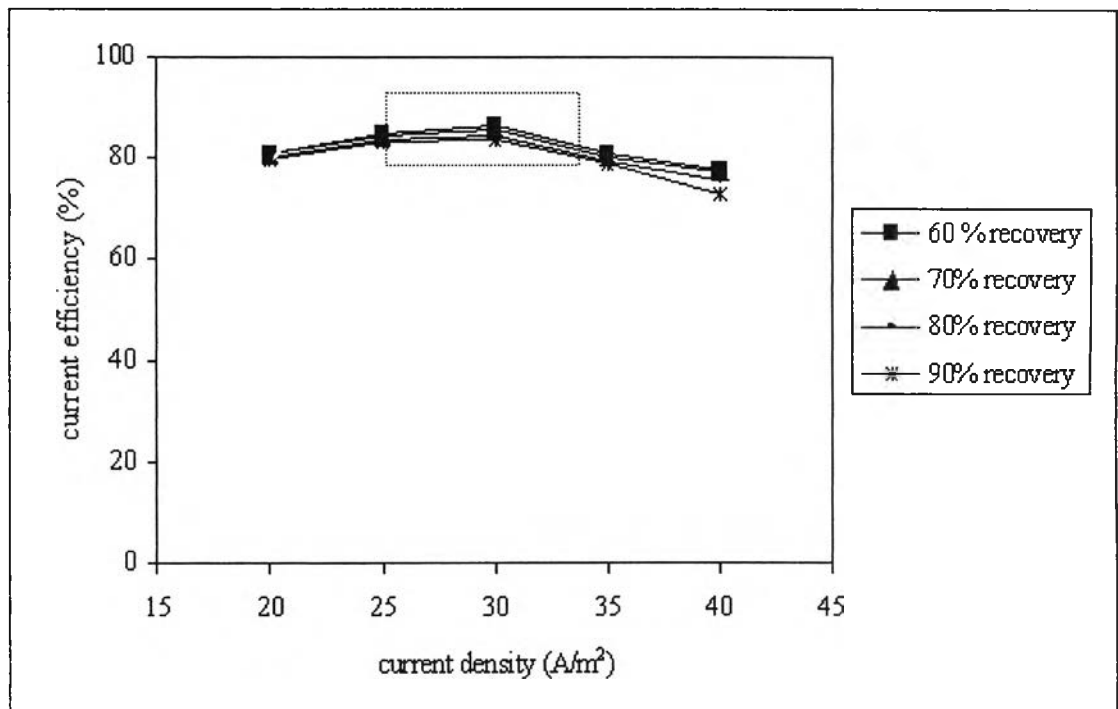Figure IV.6: Copper recovery percentage versus time (solution S3).

Figure IV.7: Current efficiency versus current density (solutionS3).

Figure IV.6 shows the results of copper recovery from the synthetic aqueous solution with 5 g/l at pH = 1 (solution S3) as a function of time (0 - 11 hours) at various current density (between 20 - 40 A/m^2). More than 70 % of copper ions contained in synthetic solution was recovered in 9 hours by applying current density between 20 - 42 A/m^2. Current efficiencies determined at every current densities are expressed in Figure IV.7. The current density which was given the maximum current efficiency (known as the optimum current density) was found between 25 - 30 A/m^2. More than 90 % of copper was recovered in 10 hours with more than 85 % current efficiency.

The current efficiency behaviour obtained from the solution with higher copper concentration gave as same tendency as from the solution of lower copper concentration. Followed this result, the following experiments at high copper concentration were performed with an applied current density of 30 A/m^2.

1.1.2 Influence of electrolyte flow rate

Phenomena in metal deposition are significantly affected by a flow rate of electrolyte. The relationship between electrolyte flow rate and rate of mass transfer is generally expressed as dimensionless number. In this study, experiments were performed at different flow rates of electrolyte. The model was built to explain the relationship between experimental concentration (C_{exp}) and model concentration (C_l) as a function of time and then the mass transfer coefficient of the system can be determined.

1.1.2.1 Experimental results

1.1.2.1.1 Low copper concentration

Various flow rates of electrolyte from 0.93 to 3.0 l/min were investigated to determine its effect at optimum current density of 10 A/m^2. Synthetic copper solutions were prepared at concentration of 1 g/l at pH = 1 (solution S1) and 1 g/l at pH = 5 (solution S2). Results of these experiments are plotted in Figures IV.8 and IV.9.
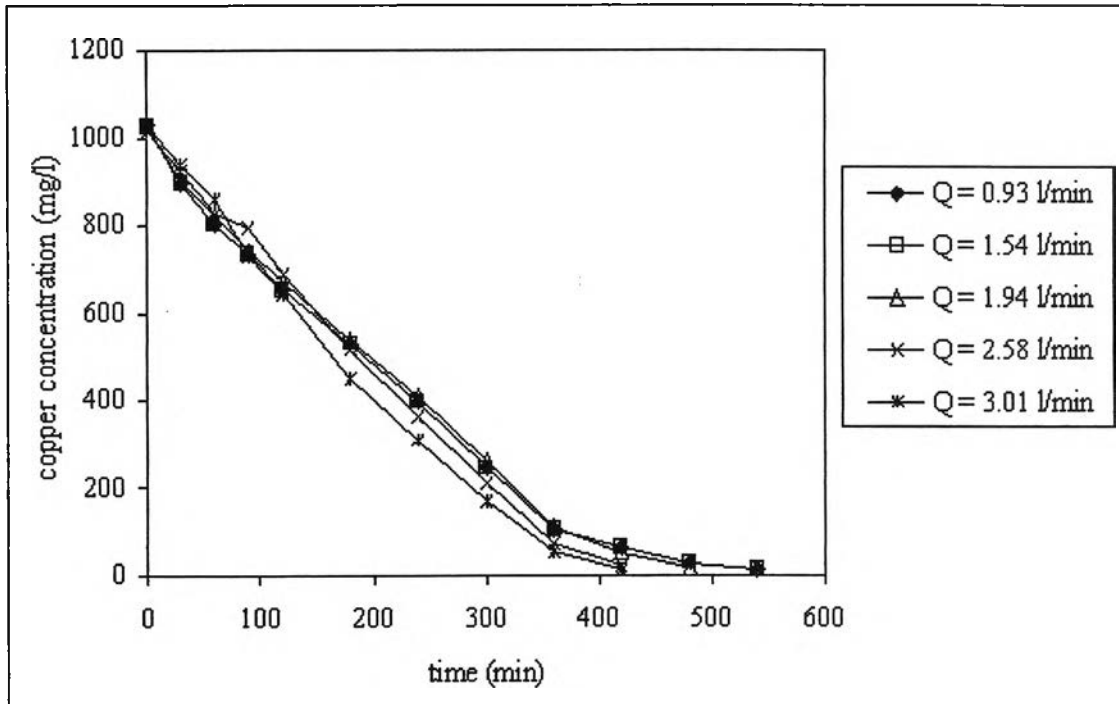
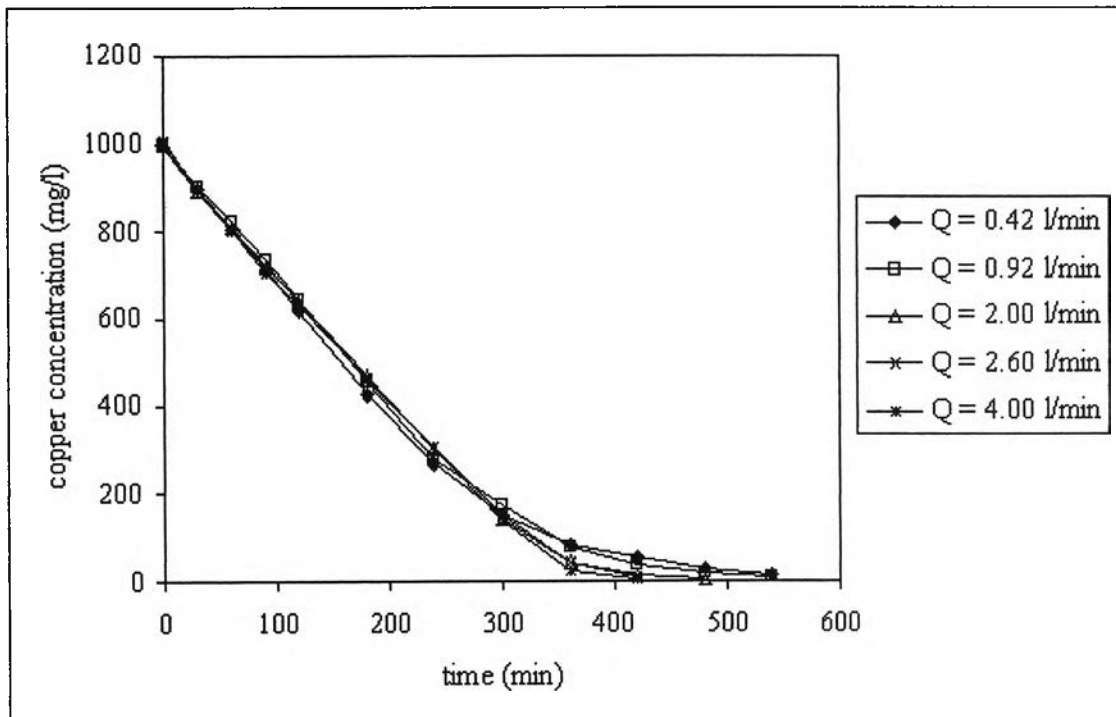Figure IV.8: Concentration evolution of copper at different flow rates (solution S1).

Figure IV.9: Concentration evolution of copper at different flow rates (solution S2).

At the beginning, the linear concentration evolution was obtained and its evolution was nearly the same at different flow rates. It can be stated that the kinetic

of the beginning step is controlled by a charge transfer which is independent of flow rate. Later, the relationship between an amount of metal ions and time is in exponential form. At this stage, the kinetic is controlled by mass transfer which depends upon the flow rate.

1.1.2.1.2 High copper concentration

Various flow rates of electrolyte from 0.42 to 4.0 l/min were investigated with high copper concentration (5 g/l at pH = 1) at the optimum current density of 30 A/m^2 as shown in Figure IV.10. A few deviations of concentration as exponential form were observed at the lowest flow rate (0.42 l/min). Beside this, the concentration evolution was in linear form. It indicated that the system was principally controlled by charge transfer, no mass transfer occurred in the system at higher flow rate. Nevertheless, the mass transfer of this system can be occurred at very low amount of active species in solution near the end of electrolysis time.

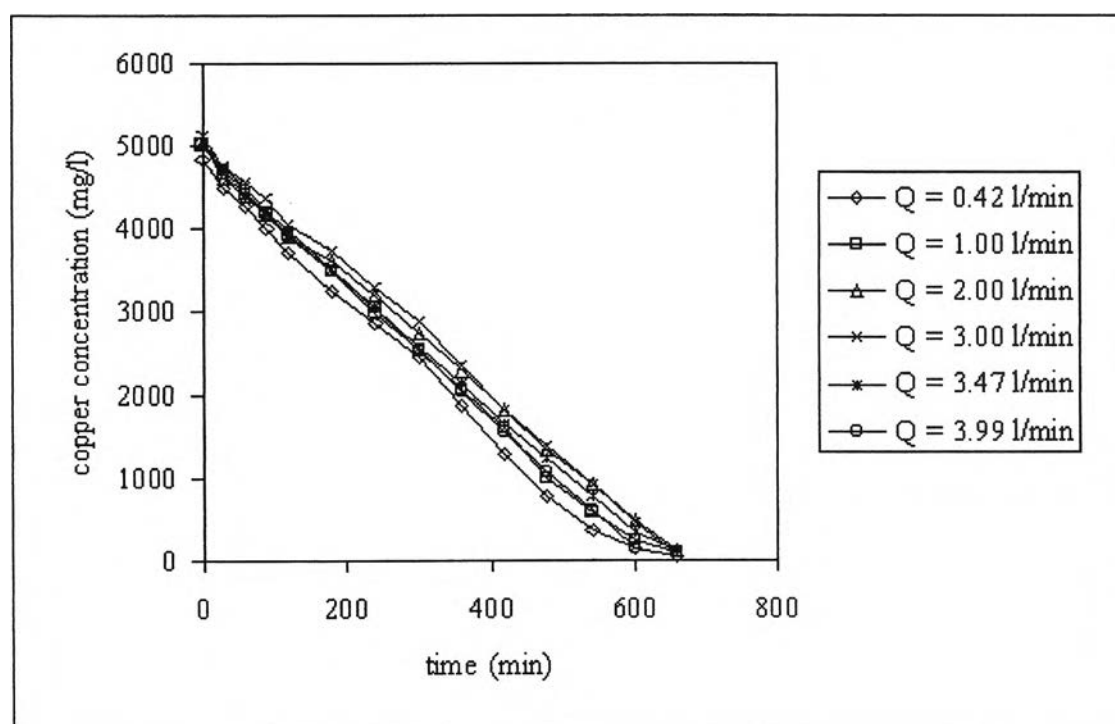

Figure IV.10: Concentration evolution of copper at different flow rates (solution S3).

1.1.2.2 Reactor modelling

This model is developed to find the relationship between the flow rate of electrolyte and the rate of mass transfer. The rate of mass transfer was calculated

from the metal concentration evolution ($C*$) versus time ($t*$). The mass transfer coefficient (k_L) was then determined from the various electrolyte flow rates. Values of $C*$, $t*$ and k_L were calculated by the following model.

The model was developed through the mass transfer of batch reactor as shown in Chapter II. The optimum mass transfer coefficient was calculated by a trial & error method that gave the minimum value of standard deviation (S) as described in the following equations.

$$S = \sqrt{\sum \left(\frac{C_1 - C_{exp}}{C_{av}} \right)^2} \tag{IV.3}$$

at $0 < t < t^*$
$$C_1 = C_0 - \frac{|j_l| a_e' t}{nF} \tag{IV.4}$$

at $t > t^*$
$$C_1 = C^* \exp\left(-k_L a_e'\right)(t - t^*) \tag{IV.5}$$

where
$$C_{av} = \frac{(C_{exp} + C_1)}{2} \tag{IV.6}$$

$$C^* = \frac{|j_l|}{nF k_L} \tag{IV.7}$$

$$t^* = \frac{(C_0 - C^*)}{|j_l| a_e'} \tag{IV.8}$$

1.1.2.2.1 Low copper concentration

Figure IV.11 shows the comparison between the evolution of experimental concentration and the model concentration as a function of time at 0.93, 1.54, 1.94, 2.58 and 3.01 l/min flow rates of synthetic solution S1 at current density of 10 A/m^2. The results obtained from the experimental and model concentrations were in good agreement with a very low standard deviation. The value of $t*$ increased when the flow rate increased.
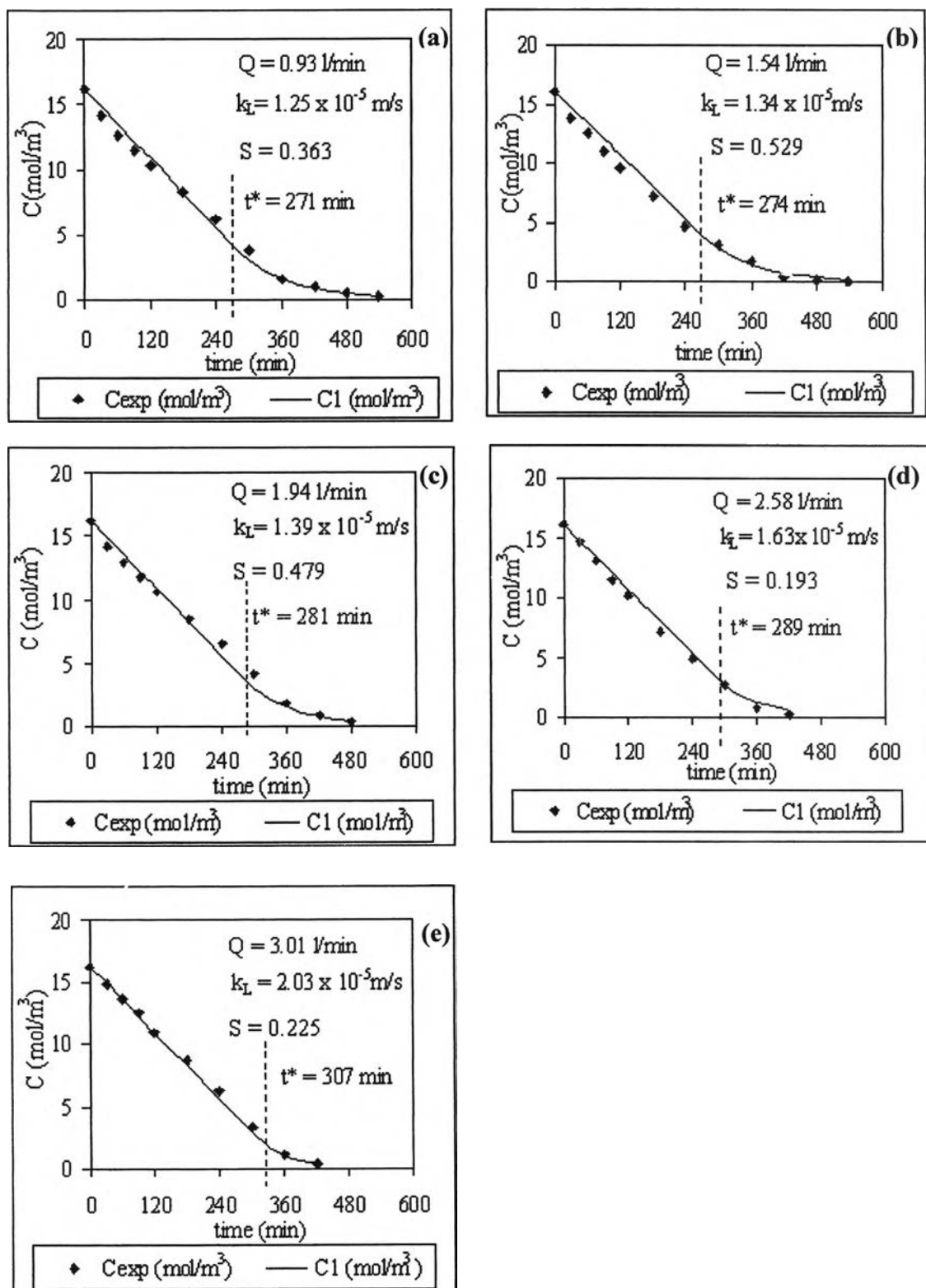
Figure IV.11: Model and experimental concentrations versus time (solution S1).

Figure IV.12 shows the relationship between mass transfer coefficients, electrolyte flow rate and Reynolds number. The evolution of mass transfer coefficient

was separated into two zones at the electrolyte flow rate of 2.4 l/min or Reynolds numbers of 363. In the 1st zone, the mass transfer coefficient was independent on the electrolyte flow rate and it was quite constant. For the 2nd zone, the mass transfer coefficient is a direct function of electrolyte flow rate.
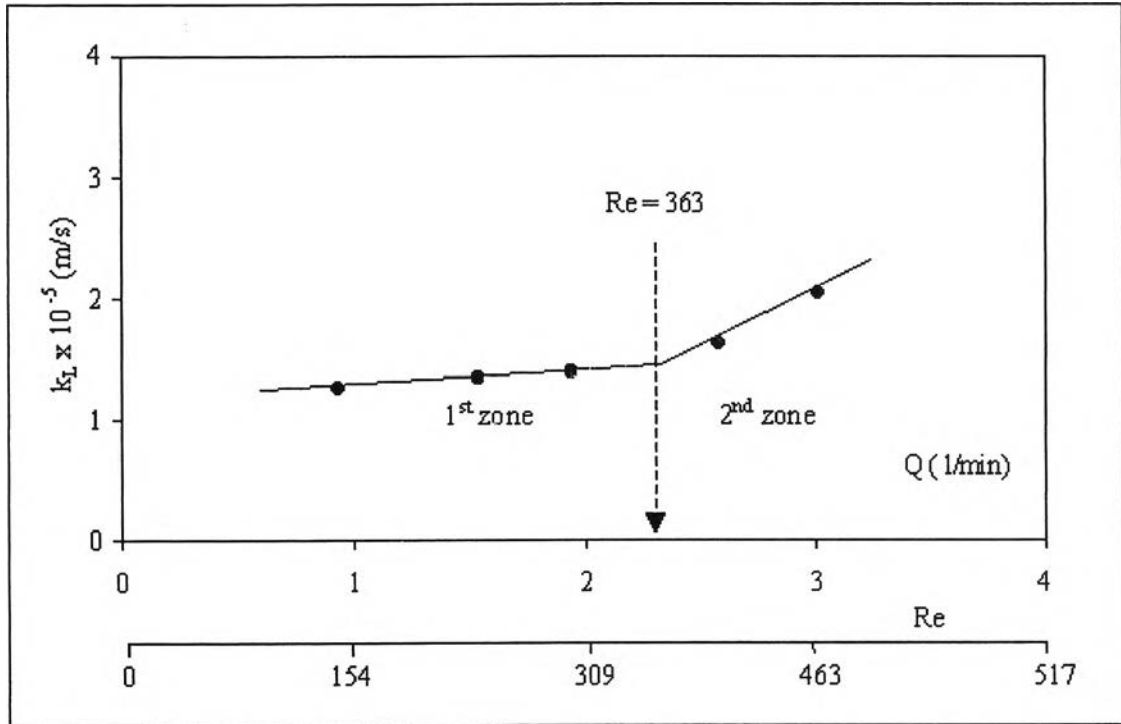

Figure IV.12: Mass transfer coefficient versus flow rates and Reynolds number (solution S1).

Such this case, a dimensionless analysis has been developed in terms of Sherwood number, Reynolds number and Schmidt number. The following relations have been established.

1st zone $Re \leq 363$ $Sh = 62 \ Re^{0.145} \ Sc^{\frac{1}{3}}$ (IV.9a)

$$= 70 \ Re^{0.145} \left(\frac{Sc \ d_h}{L} \right)^{\frac{1}{3}}$$ (IV.9b)

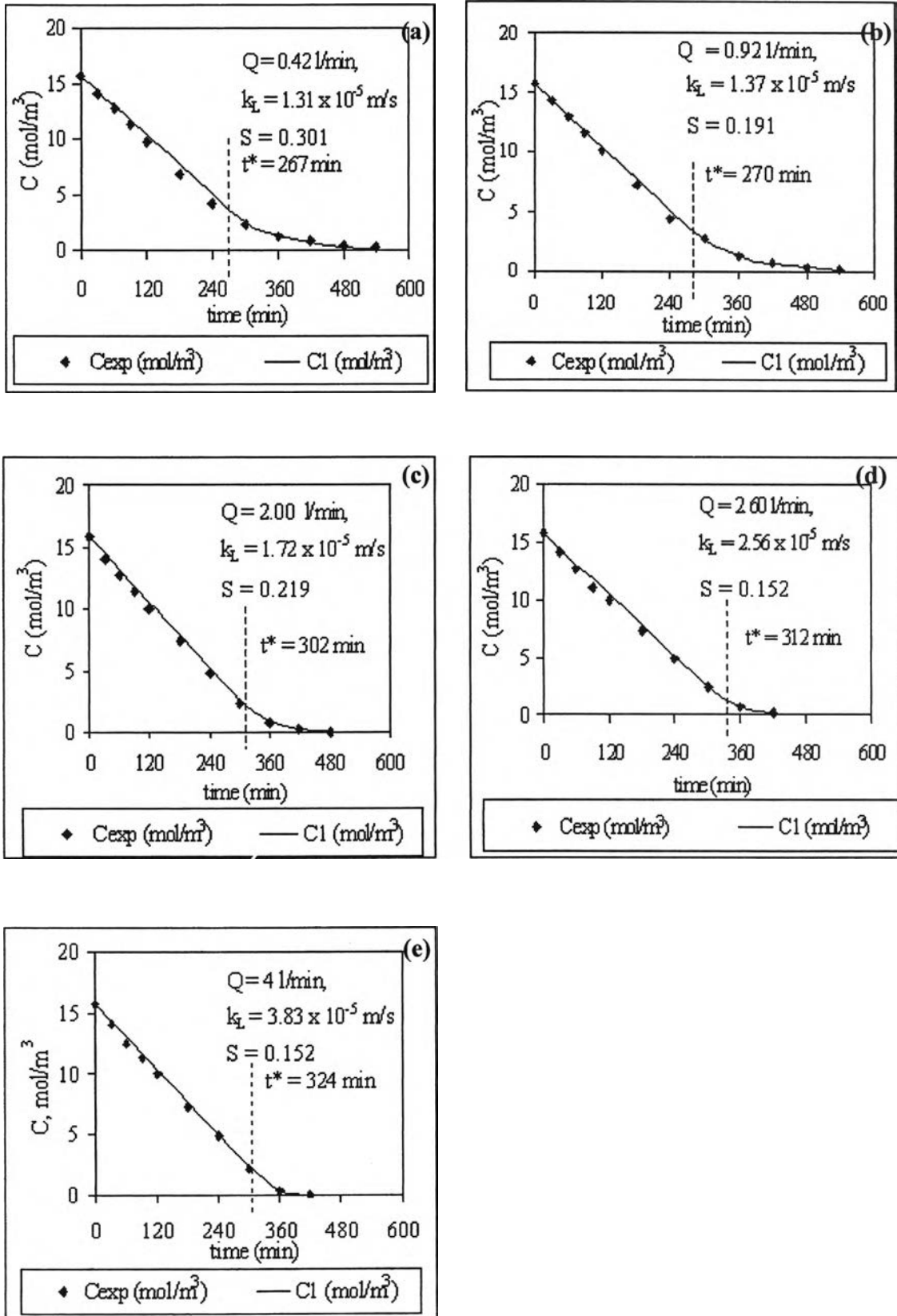2nd zone $Re > 363$ $Sh = 0.035 \ Re^{1.417} \ Sc^{\frac{1}{3}}$ (IV.10)

Figure IV.13: Model and experimental concentrations versus time (solution S2).

Figure IV.13 shows the evolution curves of experimental and the model concentrations as a function of time for solution S2 at various electrolyte flow rates. The results showed the similar behaviour as solution S1. The mass transfer coefficient and t^* increased when flow rates increased and the concentration evolution was in exponential form. The mass transfer coefficients were then plotted versus flow rates as shown in Figure IV.14.
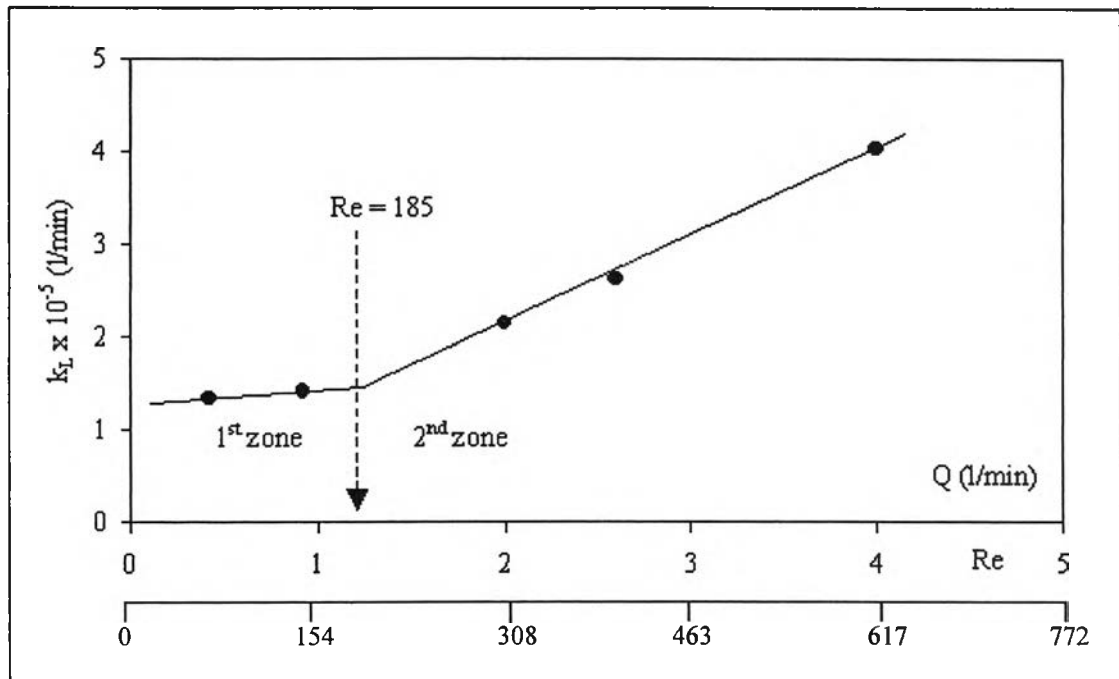

Figure IV.14: Mass transfer coefficient versus flow rates and Reynolds number (solution S2).

Mass transfer coefficients of this system were separated into two zones at Re = 185, this value is close to that obtained with solution S1. The dimensionless relations for each zone of the solution S2 were written as

1st zone $\quad\quad\quad\quad$ Re $\leq$ 185 $\quad$ $Sh = 106\ Re^{0.064}\ Sc^{\frac{1}{3}}$ $\quad\quad\quad$ (IV.11a)

$$= 120\ Re^{0.064}\left(\frac{Sc\ d_h}{L}\right)^{\frac{1}{3}}$$ $\quad\quad$ (IV.11b)

2nd zone $\qquad$ Re > 185 $\quad$ $Sh = 1.12\ Re^{0.919}\ Sc^{\frac{1}{3}}$ $\qquad$ (IV.12)

When electrolysis time is less than $t*$, the limiting step is the electronic transfer or charge transfer and the mass transfer can't be observed. Efficiency of the system equals to 100 % at all applied current in the copper electrodeposition without side reaction. At this point the slope (α) of concentration versus time curve was defined as

$$\alpha = \frac{j_l\ a_e{}'}{nF}$$ (IV.13)

for solution S1, the average slope of all flow rates was 0.0424 ± 0.0034 mol/m³s, then

$$a_e{}' = 13.64\ m^{-1}$$

$$\%\ |error| = 5$$

for solution S2, the average slope at studied flow rate was 0.0458 ± 0.0018 mol/m³s, then

$$a_e{}' = 14.72\ m^{-1}$$

$$\%\ |error| = 3$$

If the actual geometric specific area (14.3 m⁻¹) used in the system was being compared with the calculated specific surface area, the magnitude obtained from these are nearly the same. The deviations are respectively around 5 % and 3 % for solutions S1 and S2. From this point, it showed that this model is efficient to explain the behaviour of our study.

1.1.2.2.2 High copper concentration

For high initial copper concentration (solution S3), the result of electrodeposition experiments is shown in Figure IV.15. At very low flow rate, the experimental concentration evolution was in exponential form as shown in Figure

IV.15(a). Beside this figure, the concentration evolution was in linear form as a function of time. It can be inferred that the mass transfer of ions don't occur. This is because the applied current density was less than limiting current density, so the mass transfer was not direct function with electrolyte flow rate. It can be said that at high concentration, the kinetic reaction was not depending upon mass transfer of the system as low concentration, but it depended upon an applied current density. Then, it could be concluded that the kinetic reaction was controlled by mass transfer at low metal concentration and by charge transfer at high metal concentration.

The average concentration slope as defined by equation (IV.13) was calculated for solution S3. The slope was 0.1167 ± 0.0037, then

$$a_e' \quad = \quad 12.51 \quad m^{-1}$$

$$\% \, |error| \quad = \quad 13$$

When we compare between actual and calculated geometric specific area, they were nearly the same. The deviation was about 13 %. It indicated that this model was satisfactory to explain the electrochemical behaviour of copper solution with initial concentration of 1 g/l and 5 g/l.
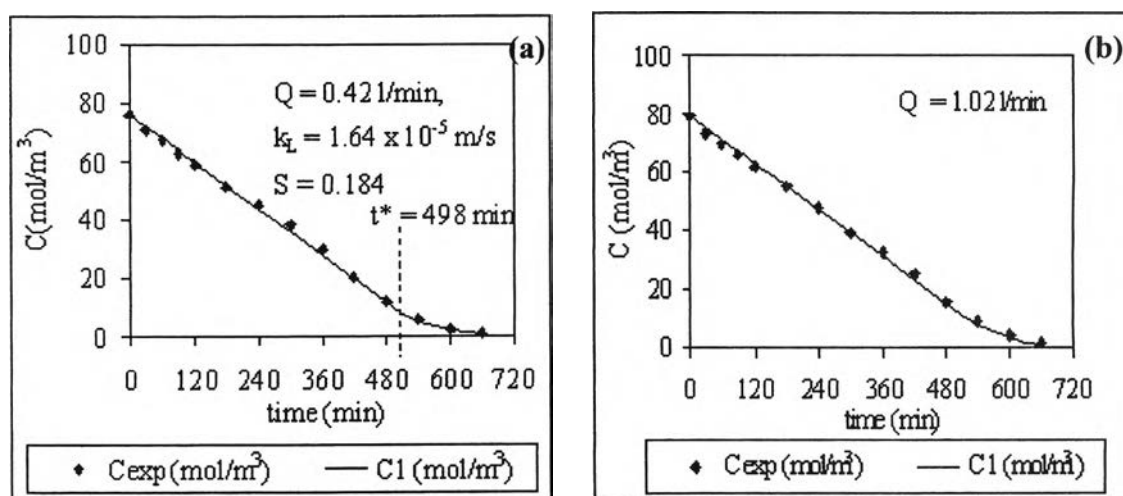

Figure IV.15: Model and experimental concentration versus time (solution S3).
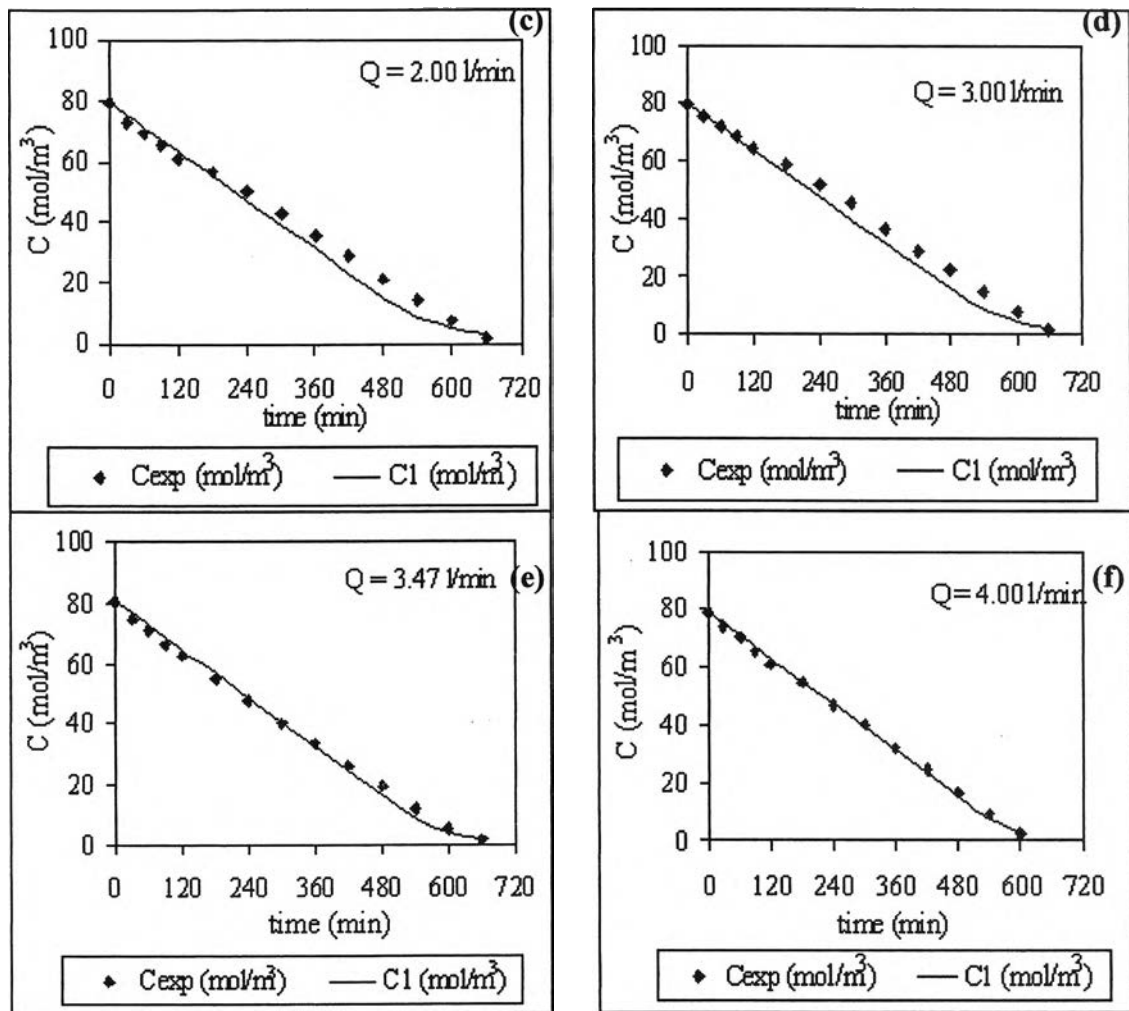
Figure IV.15: Model and experimental concentration versus time (solution S3)
(Continued).

1.1.3 Influence of initial concentration

Comparison of concentration evolution for the lower initial copper concentration (solution S1) and that for the higher initial copper concentration (solution S3) will be presented. When a metal concentration is lower than 1 g/l, the concentration evolution curves of both system have no significant difference in their rates of change (slope) as enclosed in a dashed line in Figure IV.16 and enlarged in Figure IV.17. The slopes were -0.151 (g/l)/s and -0.123 (g/l)/s for solution S1 and solution S3, respectively. It could be said that the phenomenon of solution at high initial metal concentration (5 g/l) after its concentration is less than 1 g/l is similar to the phenomenon of solution at low initial concentration (1 g/l).
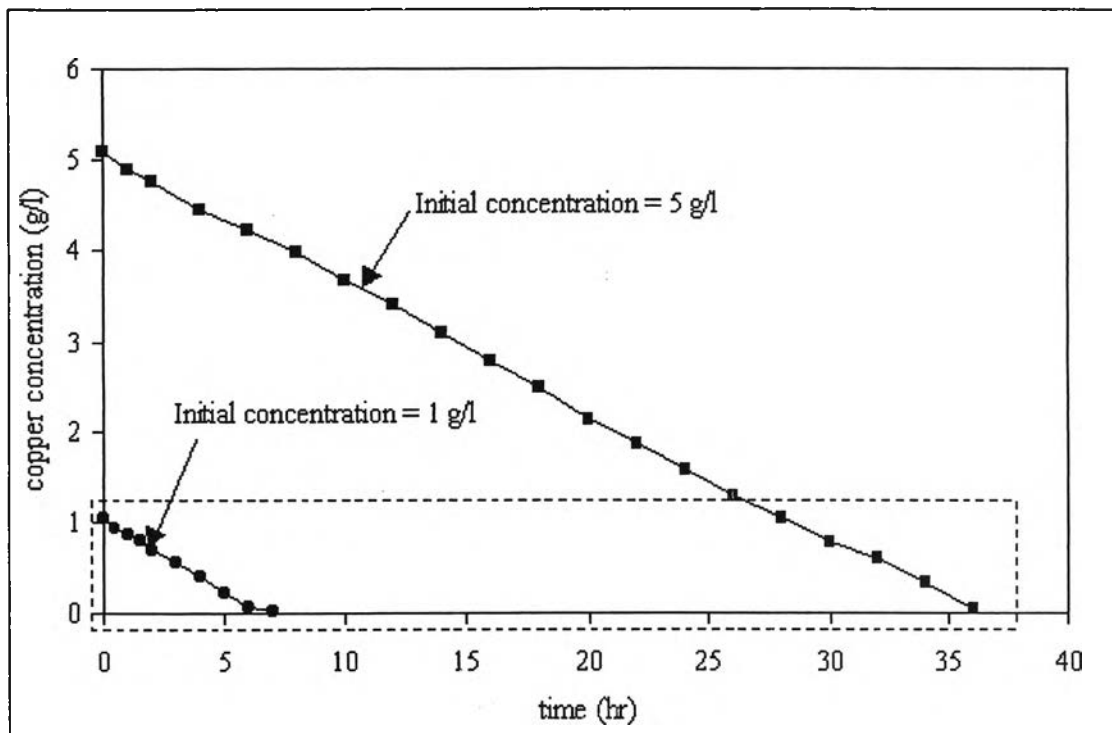
Figure IV.16: Concentration evolution versus time at current density = 10 A/m^2, flow rate = 3 l/min (solutions S1 and S3)
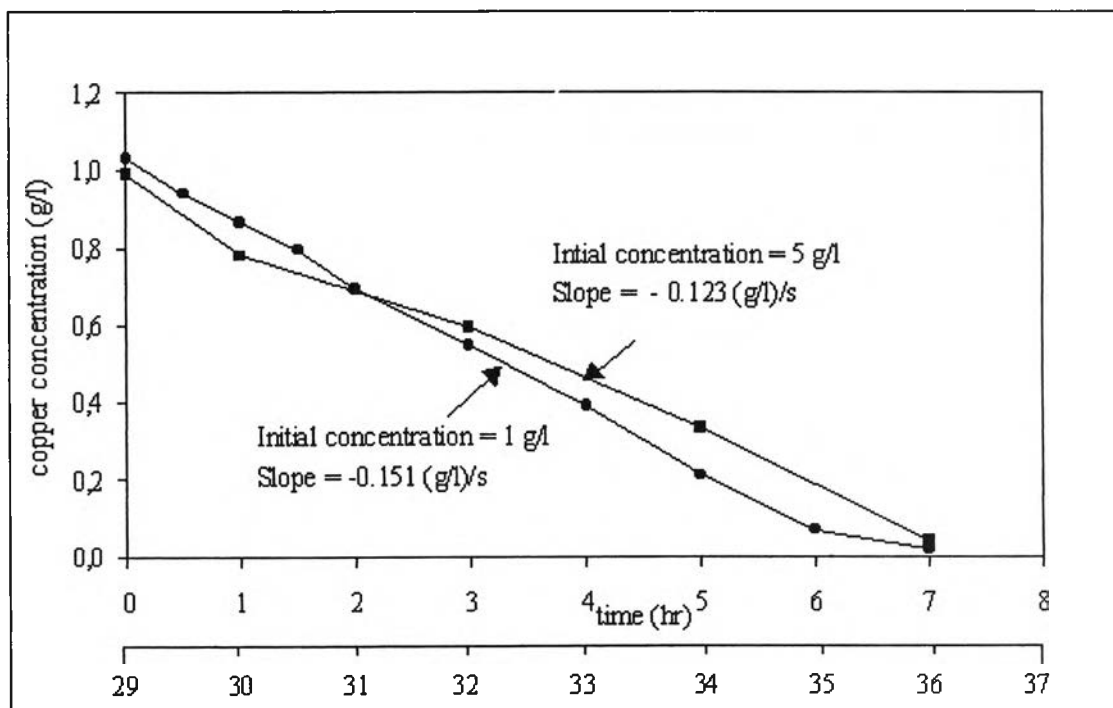

Figure IV.17: Concentration evolution versus time at concentration lower than 1 g/l (solutions S1 and S3).

Table IV.1 presents the value of mass transfer coefficient calculated by the previous developed model at low flow rate (0.42 l/min) of solutions S1 and solution S3. The results showed that the mass transfer coefficient were nearly the same for identical flow rate. It implies that mass transfer coefficient is not influenced by initial solution concentration.

Table IV.1: Mass transfer coefficient of solutions S1 and S3.

	Mass transfer coefficient (m/s)	
Electrolyte flow rate (l/min)	Solution S1	Solution S3
0.42	1.45×10^{-5}	1.64×10^{-5}

1.1.4 Compare the results with literature

Many researchers in electrochemical process attempted to develop a mass transfer coefficient in terms of dimensionless number. Table IV.2 displays the operating conditions of this work and other researchers. It consists of dimensions of reactor, dimensionless number and electrolyte properties.
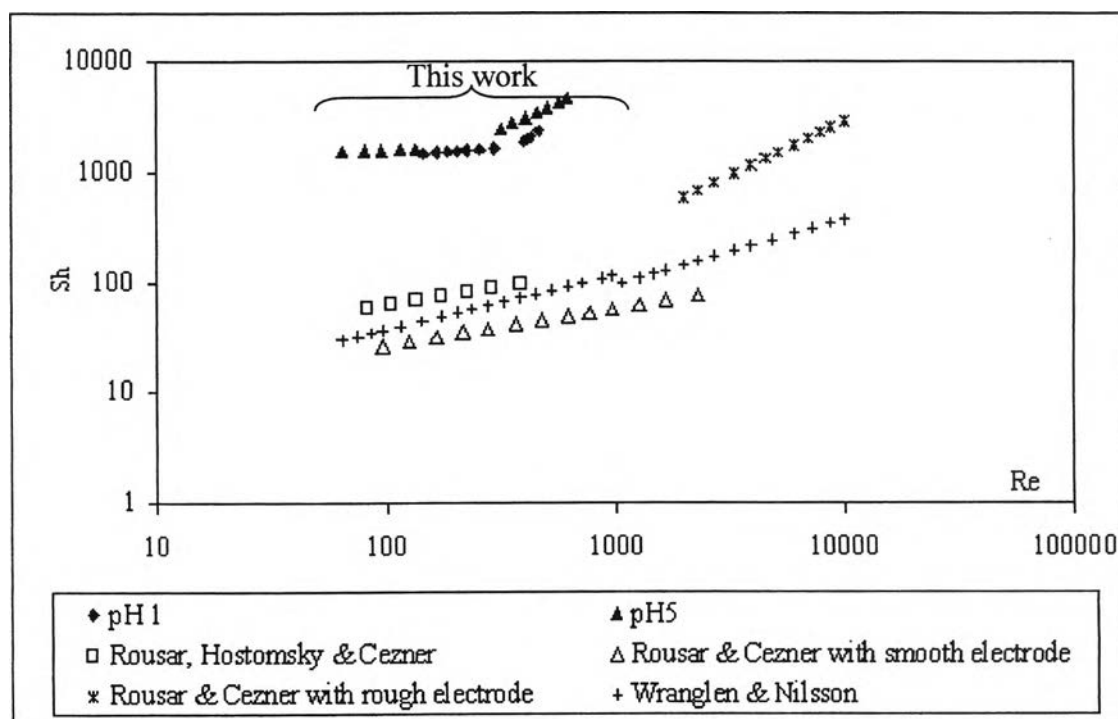

Figure IV.18: Comparison of Sherwood number and Reynolds number.

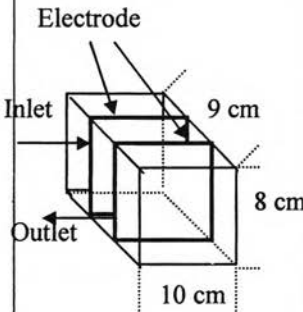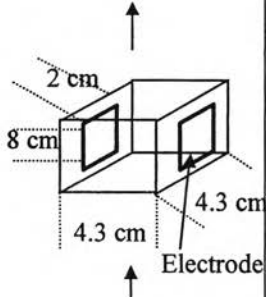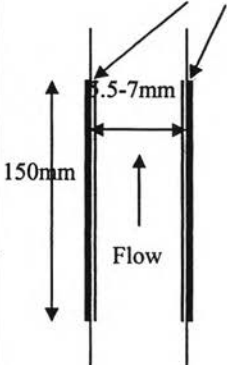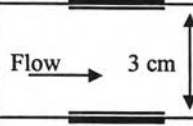Table IV.2: Comparison between literature and experimental dimensionless number.

Author / Detail	This work	Rousar I., Hostomsky, and Cezner V., [51]	Rousar I. and Cezner V., [52]	Wrangler G. and Nilsson O., [53]
Geometry	CSTR reactor $d_h = 6.84$ cm type of electrode : anode: RuO_2 cathode : Stainless steel	Flow in rectangular channel $d_h = 4.3$ cm	Flow with smooth and rough electrode $d_{hS} = 1.418$ cm $d_{hR} = 1.754$ cm size of electrode: 15x15cm type of electrode : Ni	Horizontal plane plate electrode : $d_h = 3.429$ cm electrode : Cu size of cathode : 4×10 cm^2 size of anode : 4×15 cm^2 size of cell: $4 \times 3 \times 17.5$ cm^3
Dimensionless relationship	@ pH 1 1st zone; Re < 363 $Sh = 62Re^{0.145}Sc^{1/3}$ $= 70\,Re^{0.145}(Sc\,d_h/L)^{1/3}$ 2nd zone; Re > 363 $Sh = 0.035\,Re^{1.417}Sc^{1/3}$ @ pH 5, 1st zone; Re <185 $Sh = 106\,Re^{0.064}Sc^{1/3}$ $= 120\,Re^{0.064}(Sc\,d_h/L)^{1/3}$ 2nd zone ; Re>185 $Sh = 1.12\,Re^{0.919}Sc^{1/3}$	$Sh = 1.52\,(Re\,Sc\,d_h/L)^{1/3}$ $82<Re<283$	For smooth electrode $Sh = 1.813\,(Re\,Sc\,d_h/L)^{1/3}$ $93<Re<2300$ For rough electrode : $Sh = 0.025\,Re\,Sc^{1/3}$; $2000<Re<10^4$	$Sh=0.417Re^{1/2}Sc^{1/3}$ at $Re<10^3$ $Sh=0.17\,Re^{3/5}Sc^{1/3}$ at $10^3<Re<10^6$
Electrolyte solution $D(m^2/s)$ $v(m^2/s)$ $\rho(kg/m^3)$ $T(^{\circ}C)$ Sc	$CuSO_4$ with H_2SO_4 and NaOH 5.89×10^{-10} 9.24×10^{-7} 1005.6 25 1568	Hg^{2+}, Ag^+ 7.60×10^{-10} 9.66×10^{-7} - 25 1271	0.45M $K_4Fe(CN)_6$, 0.5M KOH, 0.01M $K_3Fe(CN)_6$ 6.2×10^{-10} 1.06×10^{-6} 1123 25 ± 0.4 1709	0.75M $CuSO_4$, 1.5M H_2SO_4 9.96×10^{-10} 6.98×10^{-7} 1108 55 700

Figure IV.18 shows the correlation between Sherwood numbers and Reynolds numbers of this work and the literature. We observe that the mass transfer coefficients of our work were higher than that of other literatures at the same range of Reynolds numbers. They would be at Reynolds number of 363 which is about 5 times higher than the literature.

1.1.5 Provable experiments

The large difference of mass transfer coefficient and transition point might be due to the dimension and geometric shape of reactor. All reactors other works were channel or plug flow reactors with plate electrodes located at the reactor wall as shown in Table IV.2 whereas the reactor of this work was a simple batch reactor and electrodes were immersed in the solution. The electrolyte in the plug flow reactor contacted with only one side of electrode. However, in our case, both sides of electrode were contacted by electrolyte and the solution flow pattern promoted a turbulent condition.

Due to the large difference in mass transfer coefficient between this experiment and other works, the provable experiments were conducted to test the upper hypothesis. These experiments were performed in the batch reactor followed the procedure of Rousar and Cezner [52]. Operating conditions are shown in Table IV.2. Table IV.3 presents chemical substances and some physical properties of electrolyte used which is similar to the literature. The limiting current was measured at electrolyte flow rates of 1 to 5 l/min.

Table IV.3: Chemical and physical property of solution used for provable experiment.

Chemical substance	0.01 M $K_4Fe(CN)_6$, 0.01 M $K_3Fe(CN)_6$, 0.50 M KOH		
Physical property	Diffusivity (D)	6.20×10^{-10}	m^2/s
	Kinematics viscosity (υ)	1.06×10^{-6}	m^2/s
	Density (ρ)	1123	kg/m^3
	Temperature (T)	25	$^{\circ}C$
	Sc	1709	
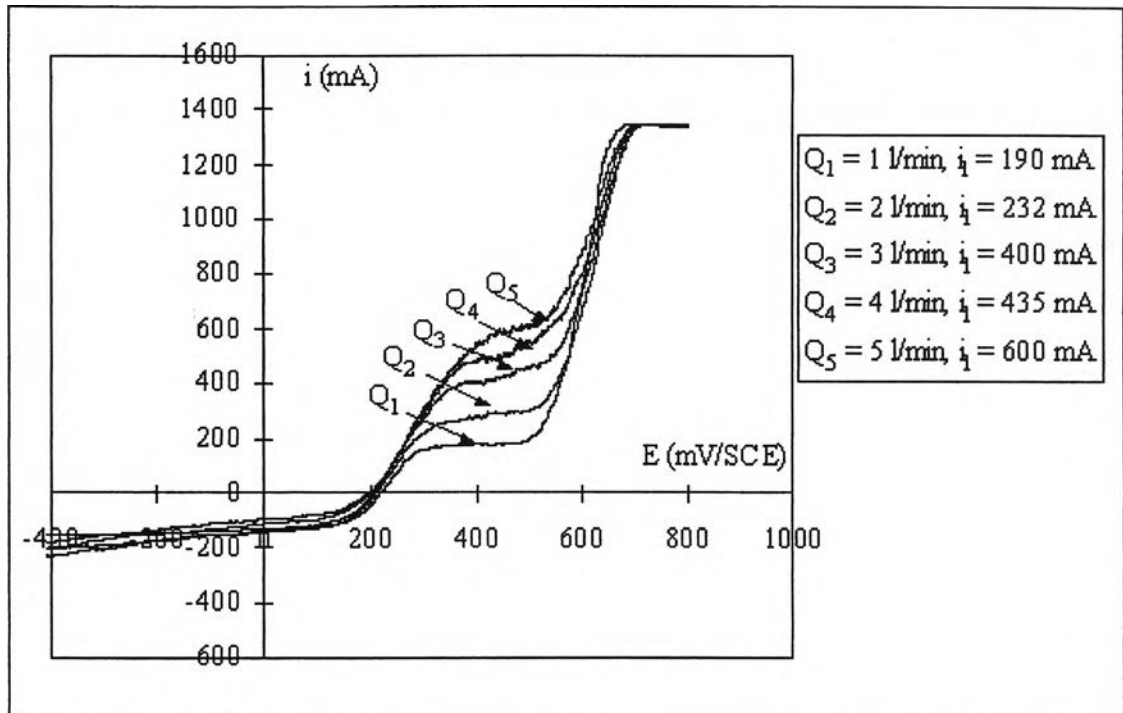
Figure IV.19: Polarization curves of provable experiments.

Figure IV. 19 shows the experimental results with different flow rates. Average mass transfer coefficients and Sherwood numbers were calculated from the following equations and are presented in Table IV.4.

$$k_L = \frac{i_l}{nFAC}$$ (IV.14)

$$Sh = \frac{k_L d_h}{D}$$ (IV.15)

Table IV.4: Results of provable experiments.

Q (l/min)	Re	i_l (mA)	k_L (m/s)	Sh
1	143	190	1.21×10^{-5}	1335
2	285	232	1.48×10^{-5}	1627
3	428	400	2.54×10^{-5}	2805
4	570	435	2.77×10^{-5}	3051
5	713	600	3.81×10^{-5}	4208

The provable experiments were performed based on the procedure of the reference work and the obtained results were the same magnitude as our previous work as displayed in Figure IV.20. It indicated that our hypothesis is reasonable in that the large differences come from the reactor geometry. So it can be concluded that the flow rate of electrolyte affects to the mass transfer in the system. Copper is recovered by electrodeposition technique with a good metal deposition on cathode surface. The effect of initial pH can be neglected.
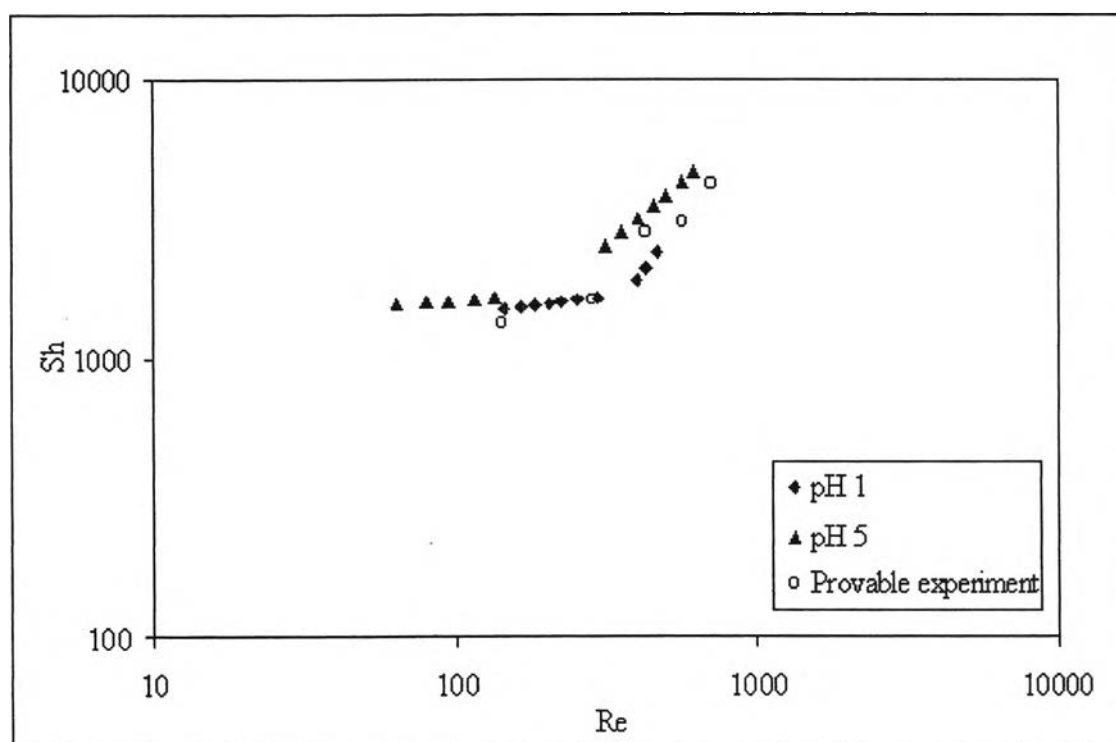
Figure IV.20: Comparison between experimental and provable results.

1.2. Copper recovery in 3PE reactor

Four parameters were studied consecutively; current intensity, air pulse frequency, type of electrode and electrolyte flow rate. All results would be presented in dimensionless group and compared with the results of other works.

1.2.1 Effect of current intensity

Experiments were preformed with synthetic copper solution which has the initial concentration of 1 g/l at pH = 1 (solution S1). The current intensity was adjusted from 5 to 11 A. Figure IV.21 exhibits the curve of copper recovery versus

time in a range of current intensity from 5 to 11 A at an electrolyte flow rate of 8.4 l/min and 0.25 Hz air pulse frequency. More than 90 % of copper ions was recovered in 4 hours by using 9 - 11 A current intensity. Outlet solution generally contained less than 1 mg/l of copper after being treated for 7 - 18 hours in operating time and current intensity from 6 to 11 A. The percentage of copper recovery was gradually increased with the current intensity up to 9 A. Beyond this point, the copper deposition had not increased on the surface of the electrode because there was a side reaction of water reduction to hydrogen gas. The limiting current intensity of this experiment would be near 9 A.
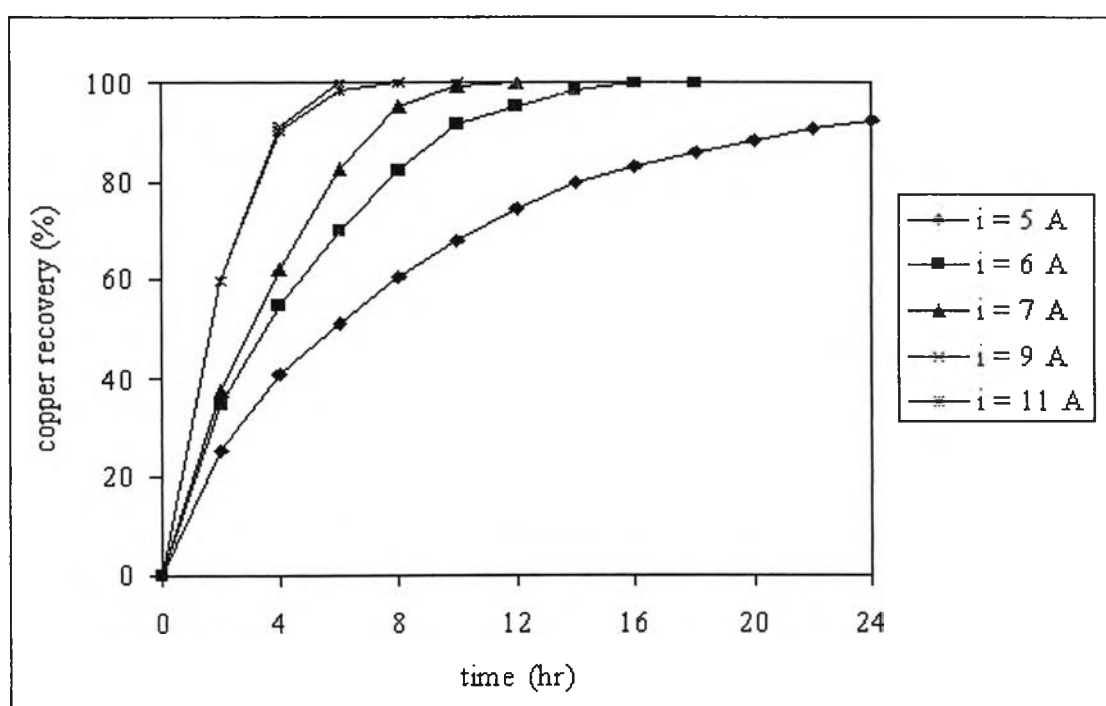

Figure IV.21: Copper recovery percentage versus electrolysis time.

In order to determine the optimum current intensity, the curve between current efficiency and current intensity is plotted and depicted in Figure IV.22. The results showed that the optimum current intensity was found at 9 A. At this point, more than 90 % of copper was recovered in 4 hours and the complete recovery was reached after 7 hours with less than 0.13 mg/l copper in the outlet solution. In addition, current efficiency was more than 30 % when 90 % of copper was recovered. From this experiment, it can be concluded that copper can be recovered at a high recovery percentage and convenient current efficiency in 3PE reactor.
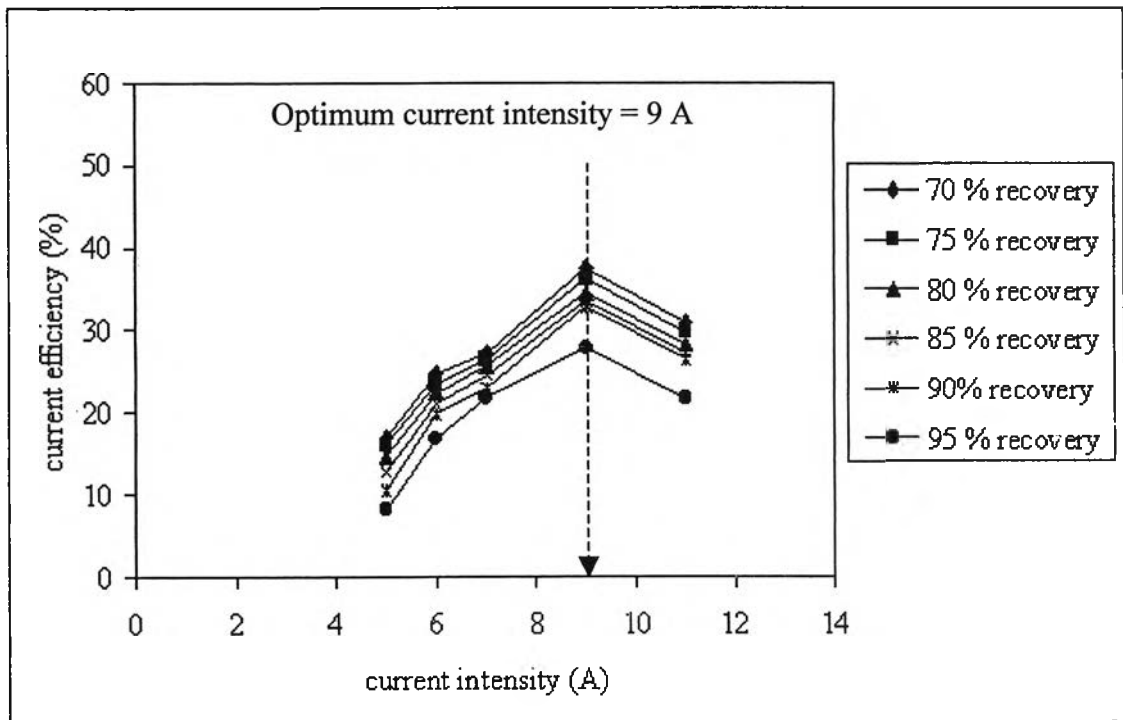
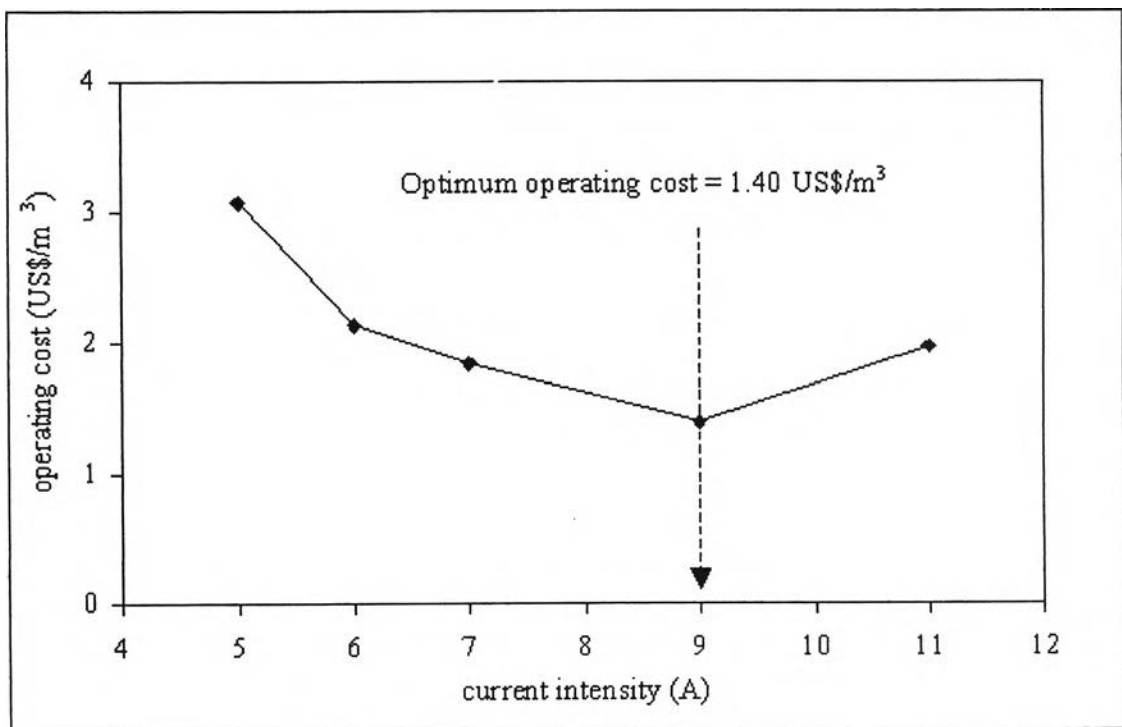Figure IV.22: Current efficiency versus current density at various percentages of copper recovery.

Figure IV.23: Operating cost versus current intensity at 99 % recovery.

The optimum operating cost which is corresponding to the lowest electricity cost was calculated in the same current intensity range. Figure IV.23 shows the relationship between operating cost and applied current intensity. The results provided that the minimum operating cost was obtained at 9 A of which corresponds to the maximum current efficiency. This reasonable cost is lower than 1.40 US$/m^3 (1 kW - hr $\approx$ 2.863 Baht or 0.066 US$).

1.2.2 Effect of air pulse frequency

In order to avoid clogging problems, electrode polarization, and dendrite formation, a periodic destabilization of granular bed by an air pulse system was applied. Some previous work [54] was focused that in order to agree with technical requirement, the pulse frequency should be less than 2 Hz.

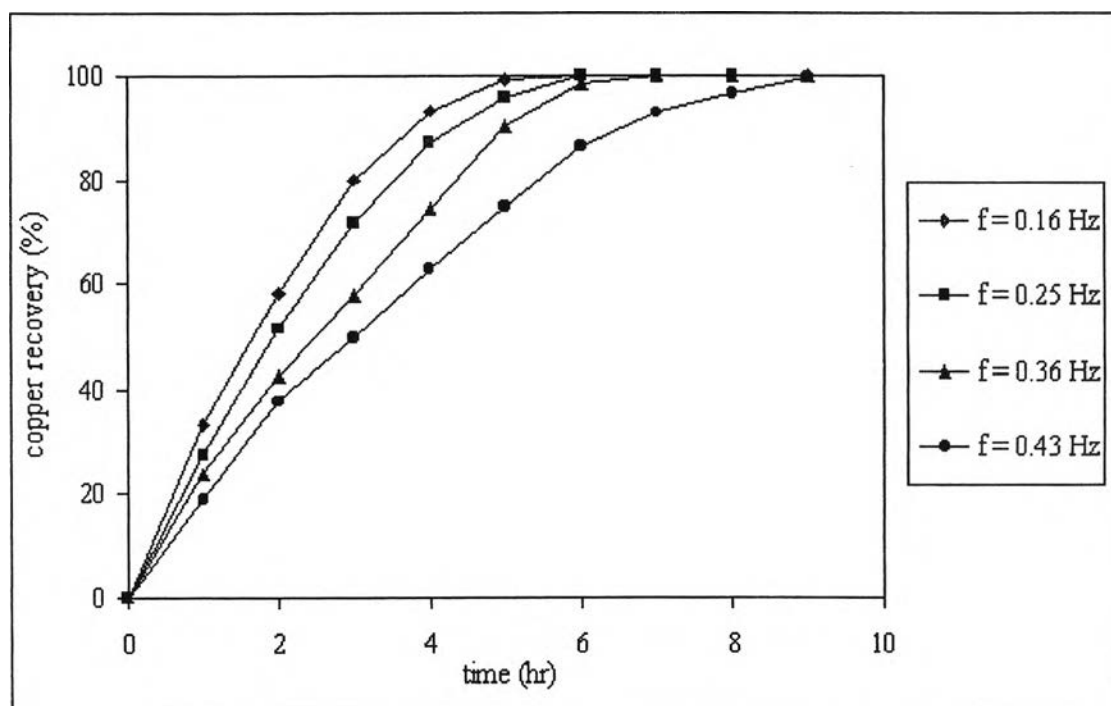Figure IV.24: Copper recovery percentage versus electrolysis time at various pulse frequency.

In this study, the pulse frequency was varied between 0.16 - 0.43 Hz at the optimum current intensity (9 A) and electrolyte flow rate of 8.4 l/min. Figure IV.24 displays the correlation between percentage of copper recovery and time in 3PE reactor with various pulse frequency. The percentage of copper recovery was changed

inversely with the pulse frequency. After 7 hours of electrolysis time, about 99.99 %, 99.91 %, 99.86 % and 92.96 % of copper ions was recovered corresponding to the outlet copper content of 0.15 mg/l, 0.94 mg/l, 1.43 mg/l and 72.45 mg/l at pulse frequency 0.16, 0.25, 0.36 and 0.43 Hz, respectively. It is due to the current intensity drop during the destabilization of graphite particles which instantaneously contact with the current feeder. When particles are fixed, the current intensity is generally constant; however, when particles are destabilized by pulsation, the instantaneous current intensity falls immediately depending on the maximum liquid velocity. From this result, decreasing of pulse frequency will promote high copper recovery. However, if the pulse frequency is less than the technical requirement ($2\pi af < 0.3$), the clogging problem may be observed.

The high contraction of the matrix is maintained at a lower pulse frequency, the better recovery rate is obtained. At pulse frequency of 0.16 Hz, the higher metal recovery was observed but the little over bridge between near particles has been observed. If the experiment was performed at pulse frequency lower than 0.16 Hz, the clogging problem will happen. For this reason, the experiment was not performed at pulse frequency less than 0.16 Hz.

1.2.3 Effect of electrode type

In each experiment, graphite particles were cleaned by nitric acid (HNO_3) to remove the deposited copper. This study is interested in the effect of the electrode nature which is consisted of fresh and clean graphite, and graphite covered by metallic copper. Experiments were tested by, firstly, performing the normal experiment similar to some previous experiments. After copper was completely recovered, a reagent of copper sulphate ($CuSO_4 \cdot 5H_2O$) was added into the solution to get an approximate concentration of about 1 g/l. Then, the experiment was continued until the complete copper recovery was again obtained.

Before performing experiments, the current density - potential curves of synthetic copper solution have been studied by using the cyclic voltammetry technique with rotating disc electrode. Two types of cathode were included; graphite and copper. The diameters of graphite cathode and copper cathode were 3.5 mm and 4 mm, respectively. Platinum grid was used as a counter electrode and a saturated calomel electrode was used as a reference electrode.
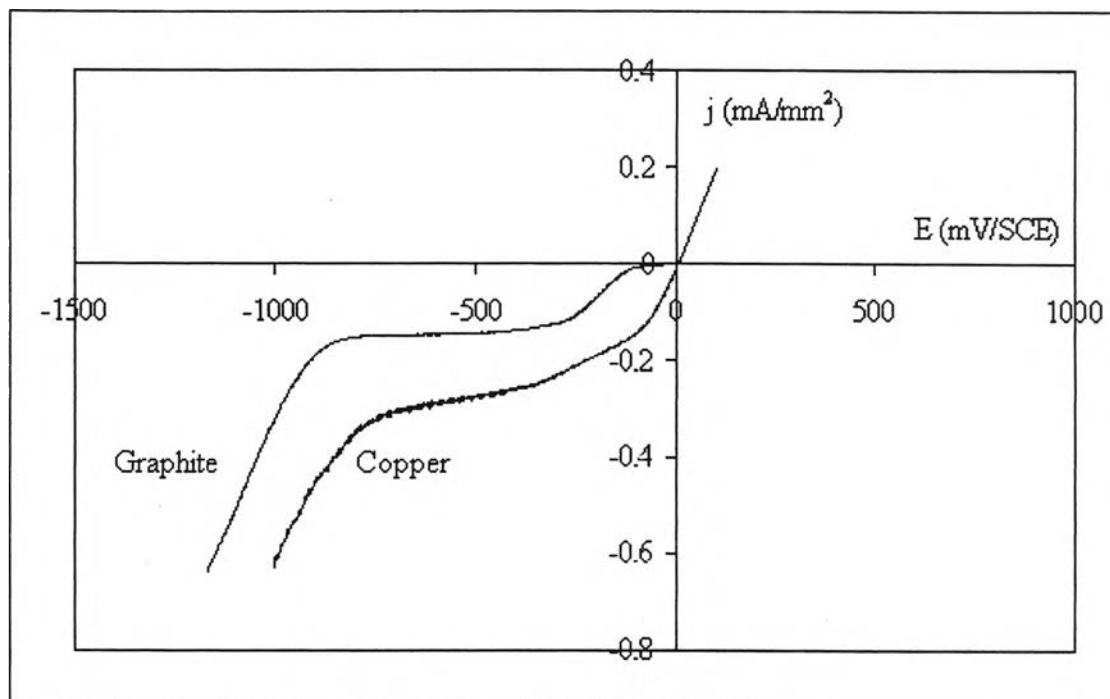
Figure IV.25: Polarization curve of copper solution with graphite and copper cathode.

The results of current density - potential curve of synthetic copper solution are shown in Figure IV.25. The reduction of copper by using graphite cathode began at a potential about -150 mV/SCE while it began at 0 mV/SCE for copper cathode. The limiting current density obtained by using copper cathode was 2 times higher than those obtained by using graphite cathode. The limiting current density of copper cathode system was around 0.3 mA/mm^2 whereas that was around 0.15 mA/mm^2 for the graphite cathode system.

If the same applied current density was employed in the study for both cathodes and this applied current density is higher than the limiting current density of both cases, the side reaction must be mainly observed in the graphite system.

Figure IV.26 illustrates the comparison between concentration evolutions and percentage of copper recovery versus time by using graphite cathode and using graphite covered by copper. The results obtained by using different cathodes condition gave the same concentration evolution and percentage of copper recovery. Copper ions were entirely removed in 7 hours with less than 1 mg/l copper in the solution for both cases. Different cathode types gave same results because graphite is quickly covered by a copper layer and then these particles act as graphite cathode initially covered by copper.
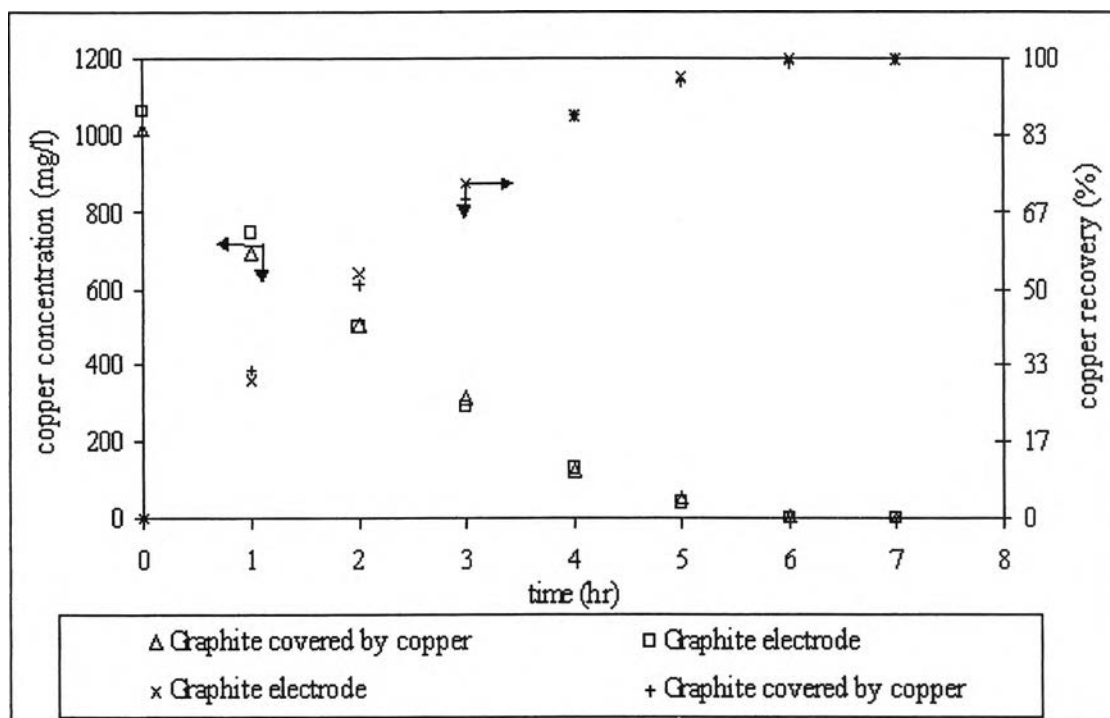
Figure IV.26: Concentration evolution and copper recovery percentage versus time for the both cathodes (graphite and copper).

From the condition used in this experiment, it can be said that copper recovery in 3PE is not affected by the cathode types including graphite or graphite covered by metallic copper.

1.2.4 Effect of electrolyte flow rate

As we had mentioned in the previous section that the electrolyte flow rate will disturb the rate of metal deposition on the electrode surface. Experiments have been performed at different flow rates ranging from 3 to 8 l/min with current intensity of 9 A and 0.25 Hz pulse frequency. The results in Figure IV.27 showed that when the electrolyte flow rate increased, the copper recovery was faster because the high electrolyte flow rate induces the high mass transfer in the system. More than 90 % of copper was recovered in 6 hours and was totally removed in 8 - 9 hours with outlet copper concentration less than 1 mg/l.
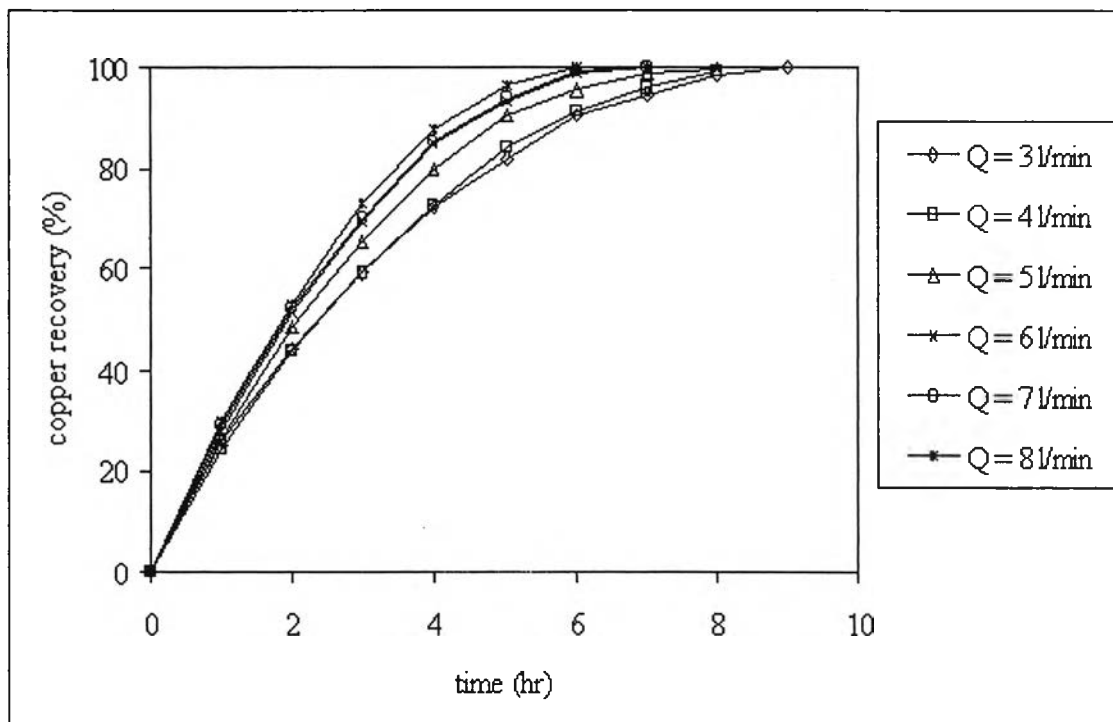
Figure IV.27: Copper recovery percentage versus electrolysis time at different electrolyte flow rates.

1.2.5 Mass transfer coefficient

The mass transfer in 3PE reactor was investigated with different flow rates of electrolyte started from 3 to 8 l/min. Concentrations used for mass transfer coefficient determination were only ranged from 50 to 1,000 mg/l because of a low precision of the analytical instrument at very low metal concentration. Figure IV.28 shows the correlation of mass transfer coefficients in a direct function of electrolyte flow rate. The mass transfer coefficient can be calculated from the dimensionless relationship of Sherwood number, Reynolds number and Schmidt number as expressed by the following equation.

$$ Sh = 1.20 \ Re_p^{0.411} \ Sc^{0.25} \tag{IV.16} $$

This relationship could be rewritten in terms of Chilton - Colburn factor (j_d) and expressed by

$$j_d = 1.20 \ Re_p^{-0.589} \ Sc^{-\frac{1}{2}} \qquad\qquad (IV.17)$$

These equations are valid in range of $6 < Re_p < 16$.
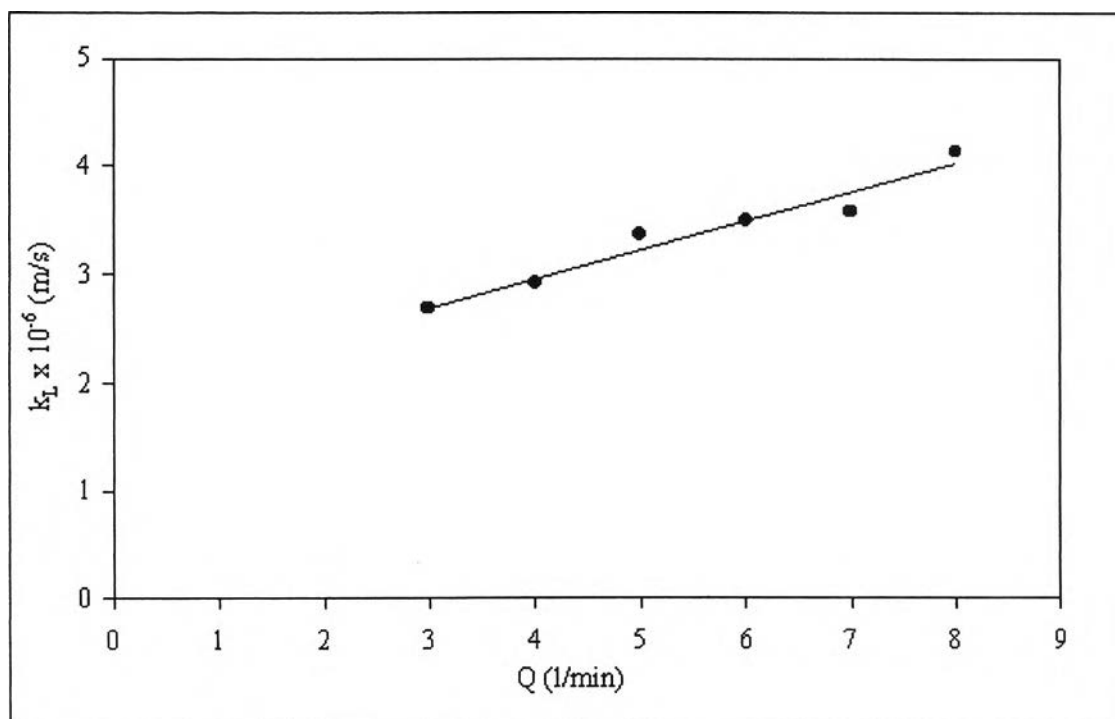

Figure IV.28: Mass transfer coefficient versus electrolyte flow rates.

1.2.6 Comparison with other works

Many researchers attempted to recover metal from processed solution by using a three - dimensional electrode. This electrode has a high specific surface area per unit volume and provides high mass transfer. This section will present a comparison between the mass transfer coefficient obtained in the current work and that found from other electrochemical systems using different three - dimensional electrodes.

Figure IV.29 shows the correlation of mass transfer coefficient $(k_L A_e)$ as a function of electrolyte flow rate in batch reactor of Panizza et al [55]. They were in a good agreement with this experiment.
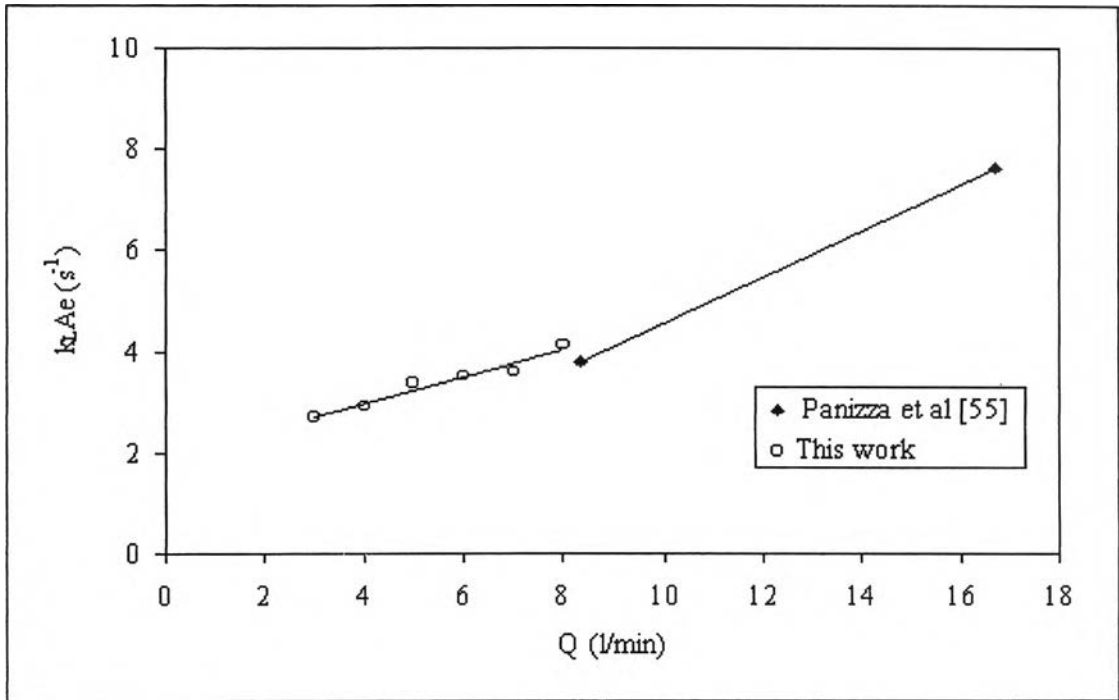
Figure IV.29: Comparison of our mass transfer coefficient with Panizza et al.
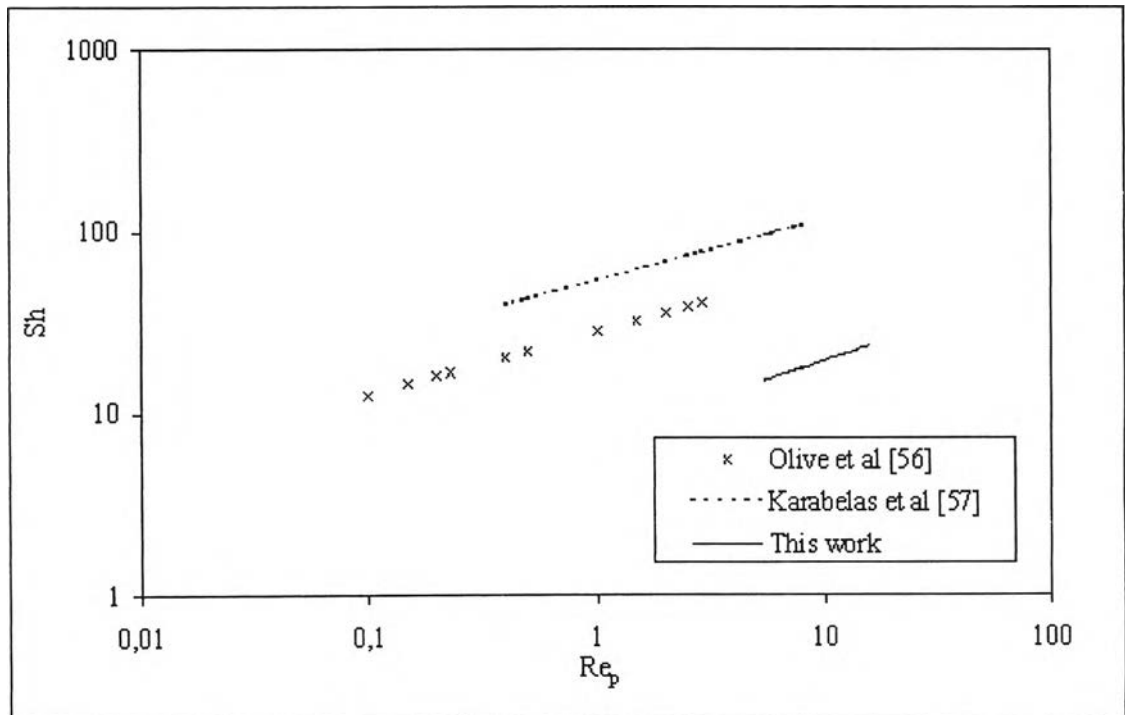

Figure IV.30: Comparison of our mass transfer coefficients with Olive et al
and Karabelas et al.

Figure IV.30 shows the results of Olive et al [56] and Karabelas et al [57]. The first work used with a flow through porous electrode in a batch system and the second work used a fixed bed electrochemical reactor in a batch process. Our results were again in good agreement with literature in the same range of Reynolds number.

2. Recovery of zinc by electrodeposition technique

The experiment of zinc recovery was set up as described in Chapter III with initial concentration of 1 g/l, pH = 1 (solution S12). The operating current density was ranged from 25.6 to 122 A/m^2. Unlike copper recovery, the experiment studied a few parameters because zinc deposition has been studied by many researchers such as Doulakas et al [44], Durairajan et al [58], Sellaf et al [59] and etc. Sellaf et al found that an optimum current density for high zinc concentration in hydrochloric solution with a high recovery percentage and a good quality of metal depositions was about 500 A/m^2 by using the copper cathode.
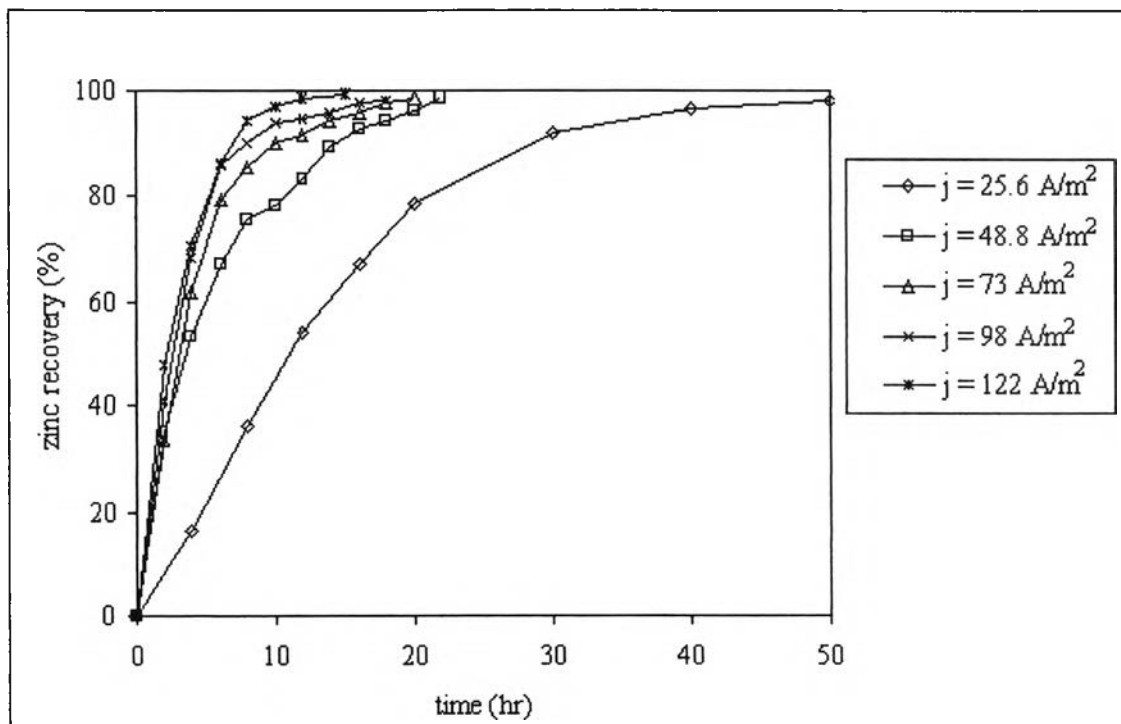

Figure IV. 31: Zinc recovery percentage versus time (solution S12).

Figure IV.31 shows the zinc recovery versus time at various current density. The rate of zinc deposition changed very rapid about 0.142 g/h at a current density of 122 A/m² and the rate would slow down after the zinc concentration was lower than 100 mg/l. More than 80% of zinc was recovered in 12 hours at a current density of 48.8 - 122 A/m² and more than 98 % of zinc content was recovered at all current density. Followed the faraday's law, current density and current efficiency was plotted as presented in Figure IV.32. The maximum current efficiency was observed at around 49 A/m² current density and about 14 % current efficiency was obtained at 90 % recovery. At this current density, more than 90 % zinc was recovered in 16 hours.
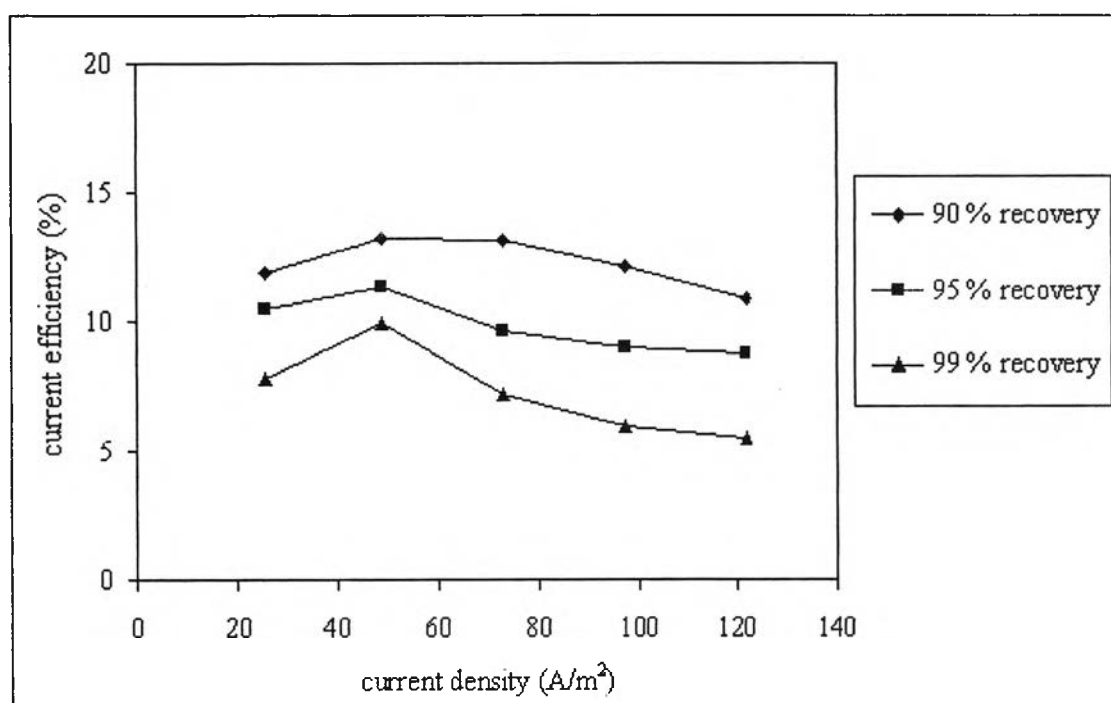

Figure IV.32: Current efficiency versus current density (solution S12).

Consider the operating cost of process, the plot between operating cost and current density is exhibited in Figure IV.33. The high operating cost was obtained at very low current density due to the slow rate of zinc deposition and the operating cost decreased when current density increased until it reached an optimum point. After that, the operating cost increased quickly when current density increased. The optimum cost for this operation was about 1.77 US$/m³. Recovery of zinc was efficient by electrodeposition technique on Zn cathode and convenient was obtained.
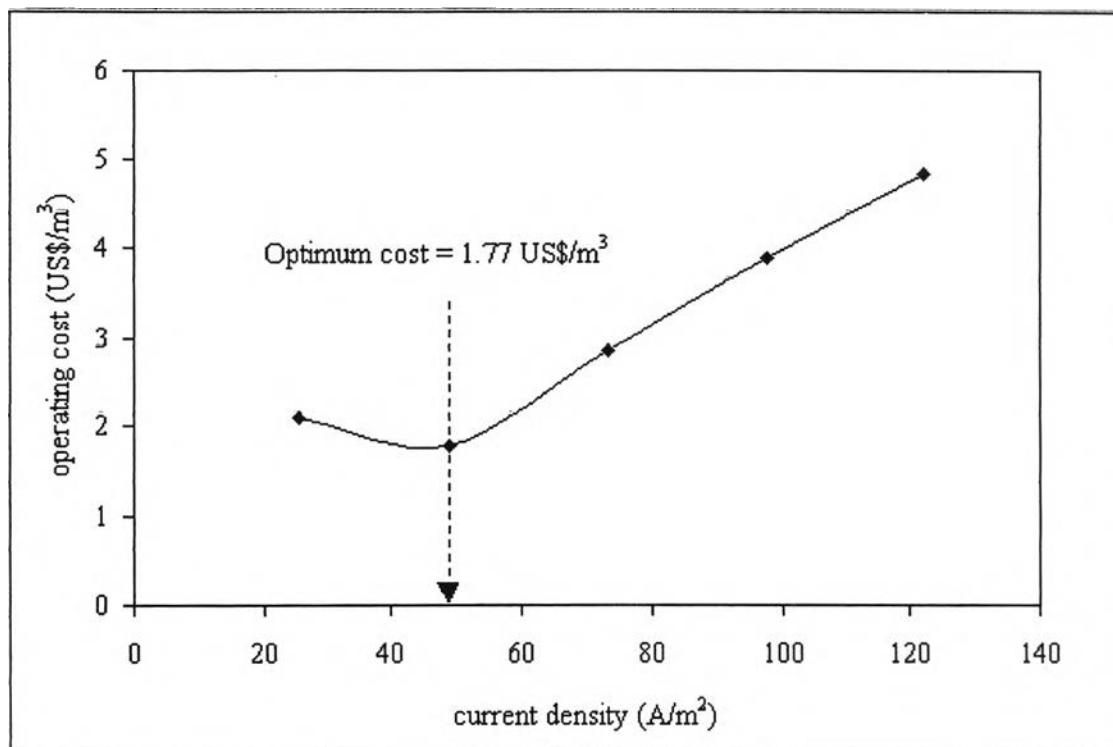
Figure IV.33: Operating cost versus current density (solution S12).

3. Conclusion

Copper and zinc containing in synthetic solutions were electrochemically recovered with a good efficiency in a reactor without membrane.

Two types of reactor were used to recover copper; a classical reactor and a modified reactor (3PE). In the first reactor, experiments had been performed with a copper concentrations of 1 g/l at pH = 1 and pH = 5 under a range of current density from 5 to 25 A/m^2 and copper with initial concentration of 10 g/l at pH = 1 with a current density from 20 to 40 A/m^2. In the 3PE reactor, experiments were carried out at a copper concentration of 1 g/l at pH =1 with a current intensity of 5 to 11 A. The investigated parameters were consisted of pulse frequency (0.16 - 0.43 Hz), types of cathode, flow rates of electrolyte (3 - 8 l/min). The results obtained in a classical reactor showed that the optimum current density for copper recovery was respectively found at 10 A/m^2 and 25 - 30 A/m^2 for low and high initial copper concentration. The kinetic reaction was controlled by charge transfer in the system with high copper concentration and by convective mass transfer in the system with low copper

concentration. The model developed to predict the mass transfer coefficient was effective to determine the behaviour of copper recovery with an error of cathode specific surface area about 5 %, 3% and 13 % for copper concentration of 1 g/l at pH = 1 and pH = 5, and copper concentration of 5 g/l at pH = 1, respectively. Our system has higher mass transfer coefficient than many other researches due to the difference in a reactor design. On the other hand, the optimum current intensity found in the 3PE reactor was around 9 A and optimum operating cost was less than 1.40 US$/m^3 with a current efficiency of more than 30 %. The recovery rate of copper was an inverse function with a pulse frequency due to the current intensity drop during the destabilization of a granular bed. Types of cathode consisted of graphite and graphite covered by copper had no effect on copper recovery. Mass transfer in the system was in a direct function electrolyte flow rate, and our dimensionless numbers were in a good agreement with those obtained from previous works.

Experiments were conducted to recover metallic zinc from synthetic solution in a classical reactor under the current density of 25.6 to 122 A/m^2 with concentration of 1 g/l at pH = 1. The optimum current density was around 49 A/m^2 with an operating cost of 1.77 US$/m^3 and the good deposited metal layer was obtained.

From this study, it can be concluded that both copper and zinc can be efficiently recovered by electrodeposition technique. However, many experiments pointed out that anomalous results such as re-dissolution, poor deposition, or precipitation can be observed at an uncontrolled pH system. In order to avoid these problems, the use of pH regulation seems to be importance and usefulness.